Theses and Dissertations--Medical Sciences

Medical Sciences

2020

Involvement of the Sigma-1 Receptor in Methamphetamine-Mediated Changes to Astrocyte Structure and Function

Richik Neogi

University of Kentucky, richik.neogi@uky.edu

Author ORCID Identifier:

https://orcid.org/0000-0002-8716-8812

Digital Object Identifier: https://doi.org/10.13023/etd.2020.363

Right click to open a feedback form in a new tab to let us know how this document benefits you.

Recommended Citation

INVOLVEMENT OF THE SIGMA-1 RECEPTOR IN METHAMPHETAMINE-MEDIATED CHANGES TO ASTROCYTE STRUCTURE AND FUNCTION

THESIS

A thesis submitted in partial fulfillment of the
requirements for the degree of Master of Science in the
College of Medicine
at the University of Kentucky

By

Richik Neogi

Lexington, Kentucky

Co-Directors: Dr. Pavel Ortinski, Assistant Professor of Neuroscience

and   Dr. Chris Richards, Associate Professor of Chemistry

Lexington, Kentucky

2020

ABSTRACT OF THESIS

Involvement of the Sigma-1 Receptor in Methamphetamine Mediated Changes to
Astrocyte Structure and Function

Methamphetamine is a highly addictive psychostimulant drug. There are currently no FDA-approved pharmacological treatments for methamphetamine addiction. Pharmacologically, (+)-methamphetamine is a dopamine releasing agent and dopamine transporter substrate that redistributes dopamine from intracellular vesicles via the vesicular monoamine transporter 2 (VMAT2) and reverses the direction of dopamine transport in the dopamine transporter. Methamphetamine, cocaine, and other drugs of abuse are also sigma-1 receptor ligands, and previous studies have demonstrated the role of the sigma-1 receptor in modulating the behavioral and cellular effects of these drugs. However, almost all these studies were conducted in cell culture systems or with emphasis on the neuronal effects of sigma-1 receptor binding.

In the literature, the sigma-1 receptor localizes robustly within neurons throughout the brain. However, there are conflicting results regarding localization in astrocytes. Here, immunohistochemical experiments were conducted on rat brain tissue containing either the nucleus accumbens or the prelimbic cortex, two brain regions critical in mediating drug-seeking behavior, in order to confirm expression of the sigma-1 receptor in astrocytes. It was determined that the sigma-1 receptor is ubiquitously expressed among neurons and modestly expressed among glial fibrillary acidic protein (GFAP)-positive astrocytes. There were no noted statistically significant differences between the proportion of cell types expressing the sigma-1 receptor in the prelimbic cortex and the nucleus accumbens. Next, the effect of methamphetamine and the role of the sigma-1 receptor on astrocytic morphology and sigma-1 receptor distribution were probed by incubating slices of striatal tissue in methamphetamine solution with or without the sigma-1 receptor antagonist BD-1063 and the sigma-1 receptor agonist PRE-084. Only the methamphetamine-treated slice exhibited a significantly different amount of stellations than the other slices. The sigma-1 receptor antagonist BD-1063 and PRE-084 abolished the redistribution of sigma-1 receptor to the processes of the astrocytes induced by methamphetamine. Thus, the data confirms that astrocytes in both the prelimbic cortex and nucleus accumbens express the sigma-1 receptor. Moreover, methamphetamine induces statistically significant redistribution of the sigma-1 receptor that is abolished by BD-1063 and PRE-084.

KEYWORDS: methamphetamine, astrocytes, sigma-1 receptor

Richik Neogi
(Name of Student)

08/10/2020
Date

Involvement of the Sigma-1 Receptor in Methamphetamine-Mediated Changes to
Astrocyte Structure and Function

By
Richik Neogi

Dr. Pavel Ortinski
Co-Director of Thesis

Dr. Chris Richards
Co-Director of Thesis

Dr. Melinda Wilson
Director of Graduate Studies

08/10/2020
Date

DEDICATION

To my parents, my PI, and my coworkers for supporting me throughout graduate school.

ACKNOWLEDGMENTS

TABLE OF CONTENTS

LIST OF TABLES

LIST OF FIGURES

LIST OF ABBREVIATIONS

IHC ……… Immunohistochemistry
PBS……… Phosphate-buffered saline
S1R……… Sigma-1 receptor
PKC……… Protein kinase C
PKA……… Protein kinase A
cAMP……… Cyclic adenosine monophosphate
DAT……… Dopamine transporter
METH……… Methamphetamine
AMP……… Amphetamine
ROS……… Reactive oxygen species
SOCE……… Store-Operated Calcium Entry
BD-1063……… 1-[2-(3,4-dichlorophenyl)ethyl]-4-methylpiperazine
PRE-084……… 2-(4-Morpholinethyl) 1-phenylcyclohexanecarboxylate hydrochloride

CHAPTER 1. MECHANISMS OF METHAMPHETAMINE ACTION

1.1 Methamphetamine as Drug of Abuse

The consequences of methamphetamine abuse place significant burden on the economy of the United States. According to a 2009 report, methamphetamine abuse cost an estimated $23.4 billion to citizens of the United States (Nicosia et al., 2009). Results from the United State National Survey on Drug Use in 2016 suggest that a significant proportion (1.6 million) of the population had used methamphetamine in the past year (SAMHSA, 2017). Moreover, methamphetamine addiction is difficult to treat due to high rates of relapse. It was estimated in a sample of patients admitted specifically for methamphetamine abuse that 61% relapsed within a year after discharge and an additional 25% during years 2-5 following discharge (Brecht and Herbeck, 2014). Additionally, methamphetamine use is increasing in the United States according to recent estimates (Jones et al., 2020). There are currently no FDA-approved pharmacological therapies for the treatment of psychostimulant abuse, highlighting the urgent need for research into the mechanisms by which psychostimulant dependence and addiction develop. Three drugs in the class of substances known as psychostimulants are cocaine, amphetamine (AMP), and methamphetamine (METH). All three drugs elevate dopamine concentrations in the ventral striatum, contributing to their reinforcing effects, yet they do so by distinct mechanisms, with AMP and METH sharing similar mechanisms of extracellular dopamine elevation. The following is a discussion of these mechanisms.

1.2 Mechanism of AMP/METH-Mediated DA Release

1.2.1 Actions at DAT

Among the psychostimulants, there are two general mechanisms of action. Drugs can either promote the release of dopamine into the synaptic cleft or they can

block the reuptake of dopamine into the presynaptic neuron. Both of these mechanisms require the dopamine transporter. The crystal structure for a humanized *Drosophila melanogaster* dopamine transporter in complex with several ligands has been solved. Both methamphetamine and amphetamine bind in a site very close to that of dopamine. The basic amine group on both molecules interacts with an aspartate residue (D46), as does the basic amine group on dopamine. Both d-amphetamine and d-methamphetamine form a hydrogen bond with the carbonyl group on the phenylalanine residue F319. That amphetamine, methamphetamine, and dopamine share very similar poses in the binding site (allowing for interaction with the transporter subsite) suggests that it is plausible that amphetamine and methamphetamine act as *substrates* for the dopamine transporter rather than simple inhibitors (Wang et al., 2015). Cocaine, on the other hand, does not allow for this interaction and can therefore be considered a pure inhibitor of the dopamine transporter (DAT). Indeed, cocaine is a classical dopamine reuptake inhibitor that stabilizes the outward-facing conformation of the dopamine transporter by binding to a site near that of dopamine in models of the dopamine transporter based on the structure of the bacterial leucine transporter (LeuT; Beuming et al., 2008).

Experiments examining the uptake of radiolabeled amphetamine into rat brain synaptosomes demonstrate that a variety of reuptake inhibitors, including methamphetamine, can inhibit the transport of amphetamine into synaptosomes, suggesting that amphetamine acts as a substrate, rather than an inhibitor of dopamine uptake (Zaczek et al., 1991) at the concentrations assayed (5 nM). The dopamine transporter is electrogenic, and transport is coupled with influx of 2 Na^+ ions and 1 Cl^- ion. This amphetamine uptake was oubain-sensitive (oubain inhibits the Na^+/K^+ ATPase), an effect that can be linked to the requirement of inward sodium flux by the Na^+/K^+-ATPase is required to maintain the concentration gradient of Na^+ and K^+. Experiments in *Xenopus* oocytes transfected with DAT revealed that cocaine can block the inward current generated by DAT. Amphetamine, on the other hand, generates an inward current, suggesting that it

drives cation transport into the cell, and the I-V plots for classical uptake inhibitors and releasing agents are distinct (Sonders et al., 1997).

Further evidence that cocaine and amphetamine/methamphetamine differ in their action at the dopamine transporter resulted from early work that demonstrated that cocaine can block the increase in blood pressure induced by tyramine, an amine that also releases catecholamines like amphetamine and methamphetamine, yet both drugs alone elevate blood pressure (Tainter and Chang, 1927). This finding was corroborated by studies in which other pure dopamine reuptake inhibitors such as benzotropine and methylphenidate could inhibit the efflux of labeled dopamine induced by amphetamine in the rat corpus striatum and in HEK293 cells expressing the dopamine transporter, respectively (Liang and Rutledge, 1982; Simmler et al., 2013). This suggests that DAT is necessary for the dopamine-releasing properties of amphetamine.

Evidence for the fact that there is more to amphetamine-mediated dopamine release than simple reuptake inhibition comes from a study that suggests that the affinity at the dopamine transporter cannot explain the behavioral potency of amphetamine (Ritz et al., 1987). In this case, behavioral potency was measured in primates. Essentially, monkeys were trained to self-administer a standard dose cocaine. Subsequently the solution was switched to contain varying concentrations of the test drug. The rate of responding to the test drug was utilized as the metric to calculate behavioral potency. The behavioral potency of (+)-amphetamine cited in this study was 0.20, similar to the drug mazindol, yet the binding affinity of mazindol is some 156 times greater than the affinity of (+)-amphetamine for DAT.

Inward transport of AMP as a *substrate* at DAT is critical for its dopamine-releasing actions. However, as amphetamine and methamphetamine are both lipophilic weak bases (meaning they can pass through the plasma membrane), it is plausible that these compounds do not require transport via DAT at higher concentrations, but rather can cross the plasma membrane by passive diffusion

(Mack and Bönisch, 1979). Moreover, the dopamine transporter does not merely act to transport amphetamine or methamphetamine into the cell; indeed, the dopamine transporter is critical for the release of dopamine observed during amphetamine treatment (Kahlig et al., 2005; Pifl et al., 1995). However, actions at the dopamine transporter cannot explain the entire picture of how AMP mediates release of dopamine. For example, if DAT alone mediates the effects AMP and its affinity for DAT is so low, then why is AMP so potent at eliciting stimulant effects? Why does a smaller dose of methamphetamine elevate extracellular dopamine in the nucleus accumbens to similar levels or even greater levels as a larger dose of cocaine (Zhang et al., 2001; Nakagawa et al., 2011), despite its markedly decreased affinity at DAT (Ritz et al., 1987)?

1.2.2   Vesicular Actions of AMP/METH

In dopaminergic neurons, synaptic vesicles are loaded with dopamine primarily by the protein VMAT2. The other vesicular monoamine transporter, VMAT1, is localized primarily in adrenal chromaffin cells and other peripheral cell types (Schuldiner et al., 1995). The operation of VMAT is driven by a proton gradient (high concentration of protons in the vesicle, lower concentration in the cytosol) that is generated by a vacuolar H^+-ATPase. Indeed, amphetamine collapses the pH gradient maintained by the vacuolar H^+-ATPase, particularly at high concentrations. However, at low concentrations the loss of the pH gradient cannot account for dopamine released from rat brain synaptic vesicles (Floor and Meng, 1996). VMAT then transports monoamines into the vesicle by transporting protons out of the vesicle; two protons are exchanged for a positively charged monoamine substrate. Given that this process is proton driven, it is plausible that certain weak bases might diffuse through the vesicle membrane and disrupt the proton gradient. Indeed, this is the case seen when adrenal chromaffin cells are treated with the weak base chloroquine, and a similar effect is observed when the vacuolar H^+-ATPase is inhibited with bafilomycin (Pothos et al., 2002). Both AMP and METH are also

weak bases and both induce redistribution of dopamine from vesicles. Thus, the weak base hypothesis of amphetamine/methamphetamine action was proposed.

The situation is not as simple as passive diffusion of amphetamine into synaptic vesicles and subsequent alkalinization of those vesicles; there appears to be stereoselectivity in terms of which isomer of methamphetamine inhibits VMAT2 more, with the (+)-isomer having greater potency (Peter et al., 1994). These findings are recapitulated in an experiment in VMAT-expressing HEK cells treated with a fluorescent substrate for VMAT; both S-(+)-amphetamine and S-(+)-methamphetamine inhibited uptake of this fluorescent substrate more than R-(-) isomers. Simple inhibition of VMAT2 cannot explain the dopamine releasing effects of AMP or METH since reserpine, an inhibitor of VMAT2, actually depletes the presynaptic terminal of dopamine, presumably by allowing dopamine to accumulate in the cytosol where it is vulnerable to metabolism by monoamine oxidase enzymes. Rather, there is evidence that amphetamine acts as a substrate for VMAT that is transported into the vesicle by proton antiport and alkalinizes the interior of synaptic vesicles. The fluorescent substrate, FFN206, was used to label vesicles in the *Drosophila melanogaster* brain revealing labeling of nerve terminals throughout the *D. melanogaster* brain. The animals were transfected with dVMAT-pHluorin, a fluorescent, pH-sensitive molecule inserted into the dVMAT protein. This allowed for simultaneous pH data and VMAT transport activity data to be recorded. Amphetamine dose-dependently increased the pH within vesicles, confirming the hypothesis that it acts as a weak base. This alkalinization was blocked for both amphetamine and methamphetamine when dDAT (*Drosophila* dopamine transporter) was knocked out, highlighting the fact that both AMP and METH are substrates for DAT. To determine whether the alkalinization of the vesicle was primarily a function of the weak base properties of AMP and METH, a substrate that could not be protonated (MPP+) was assayed. It was found that MPP+ could also alkalinize vesicles albeit with lower potency than AMP or METH. This suggests that the H^+ antiport mediated by substrate uptake is sufficient to alkalinize the vesicle (Freyberg et al., 2016). Thus, pure weak bases like chloroquine, which

lacks any affinity for VMAT2, displace monoamines from vesicles by a fundamentally different mechanism than amphetamine or methamphetamine; the unmodified weak-base hypothesis is not sufficient to account for the dopamine released by AMP or METH. Rather, AMP and METH are substrates for VMAT, and the substrate-coupled proton antiport action of these compounds is critical for alkalinization of the vesicle and subsequent displacement of dopamine (Hiranita and Freyberg, 2016). The only difference between this hypothesis and the general weak base hypothesis is that METH and AMP are also VMAT2 substrates whereas chloroquine is purely a weak base. This modified hypothesis does not preclude the possibility that AMP and METH can traverse the membrane of vesicles, but rather, it states that the primary mechanism by which AMP and METH enter the vesicle is by inward transport via VMAT2.

1.2.3   Hypotheses of AMP/METH-Mediated DA Release

The net effect of AMP/METH administration, that is, the release of DA from the presynaptic nerve terminal, cannot be explained by the actions of these compounds at VMAT, nor can simple inward transport mediated by DAT explain the observation that AMP and METH promote dopamine release. Moreover, dopamine is a substrate for the monoamine oxidase enzymes which are localized in the cytosol and in mitochondria – this means that any dopamine displaced from vesicles must rapidly exit the presynaptic terminal of the dopaminergic neuron, or it is vulnerable to degradation by monoamine oxidase enzymes (see 1.2.4 for AMP/METH interaction with MAO enzymes).

This is the basis of the facilitated exchange diffusion model of amphetamine action (Figure 1.1) which proposes that dopamine transporters bind intracellular dopamine due to the overwhelmingly high cytosolic concentration of dopamine in the presence of METH/AMP (due to displacement of dopamine from vesicles to the cytosol) and then release it to the extracellular milieu. The inward-facing conformation of the DAT would be transient due to low intracellular sodium

concentrations, but AMP, which both promotes the inward-facing conformation and increases intracellular dopamine would facilitate greater release of dopamine via DAT. This model is known as the facilitated exchange diffusion model and was initially used to describe reverse transport by the glucose transporter (Stein, 1967). As described above, a key facet of this model is that extracellular sodium concentrations are high. The presence of the sodium ion stabilizes the conformation of the dopamine transporter such that it is normally locked in its outward, extracellular-facing conformation (i.e. in the absence of substrate). When amphetamine binds to DAT, it induces a conformational change and is released into the cytosol, alongside the sodium and chloride ions. Since intracellular sodium concentrations are much lower than the extracellular concentration, the inward open conformation of DAT is transient, but if intracellular dopamine concentrations were high enough, the dopamine could bind to the inward open conformation and be transported out of the cell. The involvement of sodium in stabilizing the conformation of monoamine transporters was initially proposed by Bogdanski and Brodie in 1969 (Bogdanski and Brodie, 1969). In those experiments, it was found in rat heart tissue slices that media not containing sodium (i.e. intracellular sodium concentration is higher than extracellular sodium concentration) favored release of norepinephrine while sodium-rich media favored uptake of norepinephrine (more [3H]norepinephrine remained in the tissue in sodium-rich conditions than in sodium-poor conditions). Additionally, it was also found that potassium plays a role in the net inward flux of norepinephrine, as K^+ has an antagonistic effect on norepinephrine transport into the cell. The authors hypothesized that K^+ competes for the same binding site as Na^+. When the transporter faces inwards, the Na^+ binding site is exposed to the cytosol where K^+ concentrations are high. In the presence of high K^+, the transporter releases both the norepinephrine and the Na^+ ion.

The work of Fischer and Cho provided critical evidence for the facilitated exchange diffusion model of amphetamine action (Fischer and Cho, 1979). First, it was demonstrated that the release of [3H]dopamine by d-AMP was temperature-

dependent, suggesting that active transport is required for dopamine release. Second, it was demonstrated that dopamine release is partially saturable, suggesting that a population of a particular protein mediating (DAT) dopamine release by d-AMP. Third, the observed release was blocked by cocaine, recapitulating work suggesting that AMP requires the dopamine transporter for its function. Fourth, decreasing extracellular sodium concentrations shifted the dose-response curve of dopamine released vs. concentration of AMP to the right, meaning sodium plays a role in dopamine release by DAT. The latter finding supports the hypothesis that the sodium ion plays a role in the uptake of substrate by stabilizing the open conformation of DAT. It is important to note that increasing the concentration of intracellular sodium also facilitates efflux both in the absence and presence of AMP (Khoshbouei et al., 2003). That simply increasing intracellular sodium can increase efflux contradicts the facilitated exchange diffusion hypothesis because this suggests that there is no requirement for inward transport in order to promote efflux. Experiments utilizing the *Drosophila melanogaster* dopamine transporter (dDAT) co-crystallized with Na^+ suggest that Na^+ alone promotes a transition from the apo (completely unbound state) state to the outward open state in which the substrate binding site is exposed. Binding of Na^+ also stabilized the inner gate of dDAT and destabilized regions involved in promoting the outward open configuration of DAT. When dopamine is bound to the Na^+-bound dDAT, dDAT favors an outward closed conformation. This suggests that dopamine and sodium binding are prerequisites for transition to the closed conformation (Nielsen et al., 2019). The results from Khoshbouei and coworkers suggest that these properties are retained in the inward-facing conformation. Importantly, because the concentration of Na^+ is lower intracellularly than extracellularly, the stabilized, inward open conformation is transient. However, due to elevated intracellular dopamine, the likelihood of dopamine binding to the inward-facing open conformation is increased despite the lower Na^+ concentration in the cytosol.

High

Na$^+$

Low

Na$^+$

Apo
DAT

Na
DAT

Na+
AMP
DAT

Inward-
Facing
Bound

Inward-
Facing
Apo

Inward-
Facing
Na-DAT

Inward-
Facing
Bound

Outward
-Facing
Apo

Intracellular DA Increases
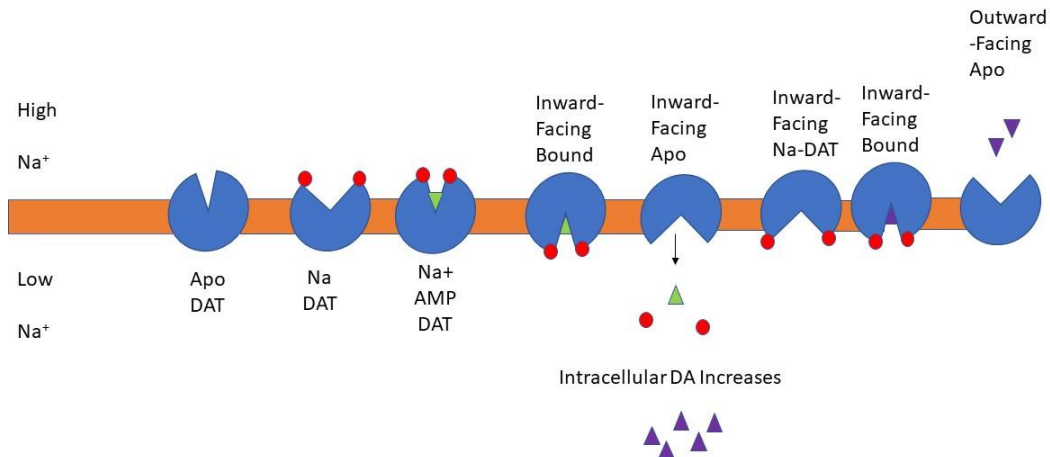
Figure 1.1 The facilitated exchange diffusion model. The red circles represent the sodium ion, the green triangles, amphetamine, and the purple triangles, dopamine. Binding of sodium to the unbound state of DAT (Apo-DAT) induces a conformational change that allows dopamine or amphetamine to bind to its binding site on the dopamine transporter. A series of conformational changes occur in the structure of DAT which results in inward transport of dopamine. The inward-facing conformation of DAT binds intracellular sodium and dopamine. In this model the elevated intracellular concentration of dopamine mediated by AMP actions permits dopamine binding to the inward-facing, sodium-bound conformation of DAT. Once dopamine binds, DAT undergoes a conformational change, releasing dopamine to the extracellular space.

Dopamine efflux mediated by injection of dopamine into the giant dopaminergic neuron of *Planorbis corneus* (pond snail) can be blocked by dopamine transporter inhibitors such as nomifensine, suggesting that the dopamine transporter mediates both efflux of dopamine from the neuron and also influx of dopamine into the neuron. This suggests that increased intracellular concentration of dopamine, perhaps that induced by dopamine redistribution from vesicles due to the action of AMP on VMAT, is sufficient to promote release of dopamine through the dopamine transporter. In other words, despite lower intracellular Na$^+$ concentration, an elevated concentration of intracellular dopamine is sufficient to promote binding to the inward-facing conformations of DAT. In the same study, amphetamine was injected directly into the giant dopaminergic neuron, and this

dramatically increased the concentration of cytosolic dopamine. Moreover, as expected, amphetamine decreased the quantal size in PC12 cells, measured by evoking release with KCl (Sulzer et al., 1995). The facilitated exchange diffusion model assumes that AMP binds to DAT and induces an inward-facing conformation due to inward transport. Because dopamine release occurred even when amphetamine was directly injected into the cell, the facilitated exchange diffusion model cannot explain dopamine release in these experiments.

Other hypotheses have emerged to explain dopamine efflux mediated by AMP. The advent of rapid patch clamp technology has enabled researchers to observe very rapid, large events that are not stoichiometrically associated with substrate translocation (i.e. the magnitude of the charge movement exceeds that associated with substrate transport). This uncoupled ion conductance has been observed for monoamine transporters such as SERT (Mager et al., 1994) and DAT (Sonders et al., 1997). The existence of these uncoupled currents suggests a channel-like mode of conductance in DAT. It has been suggested, based on outside-out patch clamp experiments in HEK293 cells stably expressing hDAT, that this channel-like conductance is also associated with the efflux of dopamine induced by amphetamine (Kahlig et al., 2005). In other words, amphetamine promotes this channel-like mode of conductance and this state of the dopamine transporter promotes bursts of dopamine release via DAT in the presence of AMP. It is important to note that much slower events were also observed; the authors termed these slower events as "transporter-like behavior." This transporter-like behavior was suggested to be associated with reversal of the direction of transport by DAT. In contrast, the "channel-like" behavior was characterized by rapid burst-firing events. Both of these observed behaviors were shown to be responsible for dopamine efflux. The channel-like events could be blocked completely by cocaine and cannot be evoked by extracellular dopamine. It was also found that intracellular Na^+ is a requirement for these channel-like events and that in the presence of intracellular Na^+ and AMP, the open probability of the DAT channel was increased. Further evidence for the connection between these rapid burst-like events and the

channel-like properties of DAT was found in comparing the channel flux ratio (ions transported per molecule of dopamine in the channel-like mode) with the transporter flux ratio (ions transported per molecule of dopamine in the transporter-like mode); the channel flux ratio is substantially higher than the transporter flux ratio. This is to be expected, since the channel-like mode of transported does not necessarily require ion binding to the transporter, so the number of ions that can pass through is increased. Apart from this channel-like mode of dopamine transport, there is another hypothesis for how AMP mediates the release of dopamine from neurons via DAT: by direct modification of DAT itself.

The dopamine transporter contains several serine/threonine residues that can be phosphorylated, and this phosphorylation could potentially regulate efflux of dopamine mediated by AMP. Experiments in PC12 cells suggest that phosphorylation by PKC drives downregulation of DAT at the plasma membrane and that phosphorylation by PKC leads to reversible internalization of DAT – phosphorylation by PKC leads to trafficking to recycling endosomes (Melikian and Buckley, 1999). It has also been demonstrated that inhibition of PKCβ as well as the canonical PKC isoforms (α, β1, β2, and γ) can inhibit efflux of dopamine mediated by amphetamine in HEK293 cells transfected with DAT. Moreover, it was found that $PKC\beta_1$ and $PKC\beta_2$ are associated with DAT and overexpression of $PKC\beta_2$ enhances AMP-mediated dopamine efflux (Johnson et al., 2005). However, PKCβ requires activation by some intracellular or extracellular signal. How can METH or AMP stimulate PKCβ to facilitate dopamine efflux? One possibility is that another receptor, one which binds METH and AMP, activates PKC, thus mediating dopamine efflux.

METH and AMPH are agonists of a receptor in the family of receptors known as trace amine-associated receptors (TAARs). The receptor known as TAAR1 is most relevant to the action of METH and AMP (Liu and Li, 2018). The endogenous ligands for this receptor are trace amines such as octopamine and p-tyramine. As phenethylamines, these compounds are structurally similar to AMP

and METH. In HEK293-DAT cells transfected with rhesus monkey TAAR1, both METH and dopamine stimulated cAMP production mediated by TAAR1 (Xie and Miller, 2007). It was observed that there was an abrupt halt in [^{3}H]dopamine uptake in the presence of TAAR1, DAT, and dopamine. This abrupt halt could be prevented by PKA and PKC inhibitors. A mutation of residue (T62D) of the DAT induced efflux of dopamine, suggesting that phosphorylation of this threonine residue can promote a conformation of the DAT amenable to efflux of dopamine (Fraser et al., 2014). Additionally, it was observed that both dopamine and methamphetamine can increase efflux of [^{3}H]dopamine in the presence of TAAR1 and DAT but not in the presence of DAT alone. This efflux could be blocked by methylphenidate or a PKC inhibitor, in the case of METH. High intracellular concentrations of dopamine mediate efflux through a PKC-independent mechanism. That METH could not evoke dopamine efflux in the absence of TAAR1, suggests that TAAR1 plays a critical role in METH-mediated dopamine efflux.

These results were recapitulated in studies utilizing WT and TAAR1-/- mouse synaptosomal preparation as well as rhesus monkey synaptosomal preparation: METH decreased uptake significantly in the WT and rhesus preparations while it did so much less in the TAAR -/- preparation. This uptake inhibition could be blocked by inhibitors of PKC and PKA. Dopamine release was first measured in HEK293-DAT cells. The results suggested that only when HEK293-DAT (i.e. not expressing TAAR1) cells are loaded with high concentrations of dopamine can release be evoked by METH. The PKC and PKA inhibitors blocked TAAR1-mediated effects of METH on dopamine efflux in the wildtype synaptosomal preparations and DAT-TAAR1 HEK293 cells that had been preloaded with high concentrations of dopamine. Inhibition of PKC and PKA only reduced the effect of METH on dopamine efflux in preparations from wildtype mice, with no effect observed in TAAR1-/- preparation (Xie and Miller, 2009). Thus, both experiments in culture and experiments using tissue support the hypothesis that TAAR1 induces dopamine efflux via PKC but not PKA.

Interestingly, TAAR1 activation by AMP could plausibly mediate the endocytosis of DAT via RhoA, the latter being activated by the Gα13 G-protein. TAAR1 coupled to Gα13 is localized specifically in the endoplasmic reticulum. In contrast, activation of PKA mediated by AMP via TAAR1 occurs in a broader set of compartments (Underhill et al., 2019). Indeed, robust DAT internalization mediated by methamphetamine has been observed in HEK293-DAT-TAAR1 cell culture (Xie and Miller, 2009).

Thus, there are several proposed mechanisms for AMP/METH-mediated dopamine release from presynaptic terminals subsequent to redistribution of dopamine to the cytosol. The oldest model for AMP-mediated release is the facilitated exchange diffusion model and hence there is a substantial body of experimental evidence supporting this hypothesis of AMP-mediated dopamine release. However, newer hypotheses have emerged, and these hypotheses are equally convincing as the facilitated exchange diffusion model.

1.2.4 Effects on DA Synthesis and Metabolism

Not only do AMP and METH release dopamine from the presynaptic terminals of dopaminergic neurons, they can also alter the synthesis and metabolism of dopamine. The most direct mechanism by which they do so is by inhibition of monoamine oxidase enzymes. Indeed, METH inhibits the A- isoform of monoamine oxidase (MAO-A) as well as the B-isoform of monoamine oxidase (MAO-B). This was demonstrated in crab-eating monkey brain mitochondrial monoamine oxidase (primarily MAO-B) and synaptosomal monoamine oxidase (primarily MAO-A) by utilizing β-phenethylamine as the MAO-B substrate and serotonin or dopamine (dopamine is also metabolized by MAO-B) as MAO-A substrates. In these experiments, METH was more effective at inhibiting MAO-A than MAO-B, and it was also shown that AMP inhibits these monoamine oxidase enzymes as well (Egashira et al., 1987). It has been shown that the D-(+) enantiomers of both METH (Suzuki et al., 1980) and AMP (Mantle et al., 1976) are

superior inhibitors of MAO, particularly MAO-A. The (+) isomer of amphetamine has a K_i of 33.8±4 µM at MAO-A and a K_i of 161±32 µM at MAO-B. The (+) enantiomer of methamphetamine is an inferior inhibitor of monoamine oxidase enzymes, with a K_i of 110±4 µM at MAO-A and 272±83 at MAO-B (Robinson, 1985). This inhibition of monoamine oxidases prevents the degradation of dopamine released from vesicles by METH or AMP, allowing more dopamine to be released from the neuron.

Another potential effect of AMP is that it can increase activity of tyrosine hydroxylase (TH), the rate-limiting enzyme in the biosynthesis of dopamine (Kuczenski, 1975). In neurons, it has been demonstrated that there are two pools of synaptic vesicles, the readily releasable pool (vesicles that are docked to the presynaptic membrane) and the reserve pool (a third pool, the recycling pool is less relevant to upregulating TH activity). Altering the duration of a train of action potentials allows one to distinguish between these two pools – the shorter train reveals information regarding the readily releasable pool while the longer train reveals information regarding the reserve pool. By varying these train lengths, different pools of vesicular dopamine could be interrogated using fast-scanning cyclic voltammetry. It was demonstrated in the dorsal striatum that 10 mg/kg amphetamine increases dopamine concentrations upon short trains (probing the readily releasable pool) and decreases dopamine concentration upon long stimulus trains (probing the reserve pool). In the ventral striatum, both 1 mg/kg and 10 mg/kg increased dopamine concentration for the short train and the intermediate train, indicating an increase in dopamine released from the readily releasable pool and the recycling pool. Strangely, there was no decrease in dopamine concentration in the reserve pool in the ventral striatum upon trains of action potentials. There was, however, a trend towards depletion of dopamine in the reserve pools when tonic release of dopamine was examined, supporting the hypothesis that amphetamine increases the size of pools that are primed for release while it decreases the size of reserve pools (Covey et al., 2013). Indeed, it has been demonstrated that when radiolabeled tyrosine is incubated with rat striatal slices, the dopamine that is

14

released is also radiolabeled, since tyrosine is metabolized by TH to L-DOPA and then by aromatic amino acid decarboxylase to dopamine.

This amphetamine-induced enhancement of dopamine synthesis has been demonstrated to be calcium dependent, as EGTA (a calcium chelator) injected directly into the mouse striatum inhibits the enhancement of radiolabeled dopamine synthesis by amphetamine (Fung and Uretsky, 1982). Several intracellular kinases are dependent on calcium for full activation. Therefore, it is plausible that a protein kinase stimulated by calcium (since EGTA inhibits enhancement of dopamine synthesis) is responsible for phosphorylating TH and enhancing its activity. Indeed, it has been observed that TH can be modulated by phosphorylation (Dunkley et al., 2004). It has also been demonstrated that TAAR1 can activate TH when TAAR1 is stimulated by 3-iodothyronamine (Zhang et al., 2018), meaning that TAAR1 can directly stimulate TH when stimulated. Whether TAAR1 stimulation by METH or AMP can directly activate TH is still unknown.

Thus, AMP and METH not only redistribute dopamine from vesicles to the cytosol and promote the release of dopamine, they also have effects on dopamine synthesis and metabolism. Inhibition of monoamine oxidase generates conditions favorable towards accumulation of free intracellular dopamine while stimulation of dopamine synthesis could mediate some of the longer-term effects of AMP and METH.

1.3 Astrocytes

1.3.1 General Role of Astrocytes in the CNS

1.3.1.1 History of Astrocytes

For many years, it was thought that neurons are the true workhorses of the central nervous system and that glia were literally the "glue" that held it together (the

word glia is derived from the Greek word for glue). In fact, when the concept of glia was first introduced by Virchow in 1856, glia were simply considered the substrate in which neural tissue was located. Initially, the cells that constituted glia were called a number of different names. Camillo Golgi, using his characteristic silver staining method, demonstrated that glia are a population of cells distinct from neurons. The term astrocyte was not introduced until 1895 when Michael von Lenhossék used the term to describe a subset of parenchymal glia. In fact, the cells with star-like projections and end feet encircling small blood vessels observed by Golgi were astrocytes. Late in the 19th century and early in the 20th century, it was realized that astrocytes are much more than the simple "glue" that holds neurons together. Ernesto Lugaro proposed a metabolic role for astrocytes, with their fine processes that invade synapses. Carl Ludwig Schleich proposed that astrocytes actively control the flow of information. Ramon y Cajal suggested that astrocytes regulate the vasculature in the brain by constricting or dilating capillaries. One of Ramon y Cajal's students, Fernando De Castro hypothesized that astrocytes release neuroactive substances that can modulate synaptic transmission – a precursor of the gliotransmitter hypothesis (Verkhratsky and Nedergaard, 2018).

1.3.1.2 Astrocyte Development

Astrocytes develop from other astrocytes (via mitosis; certain states, described later can promote proliferation of astrocytes), from progenitor cells called radial glial cells, and from NG2 glial cells (Verkhratsky and Nedergaard, 2018). During development, neurons and astrocytes are derived from the same neural stem cells. Once these cells have specified their fate by expressing several genes, they migrate along radial glial cells (which themselves can become astrocytes). Even after radial glial cells retract their processes (hence no longer function as scaffolds to direct cell migration), astrocytes still appear to migrate during development. When the astrocytes reach their final destination, they begin expressing GFAP. Although GFAP can sometimes be an unreliable marker of astrocyte maturation and expression levels can vary significantly, GFAP is the gold standard in the field; its expression is considered a hallmark of astrocyte identity. However, GFAP

expression varies regionally (Chai et al., 2017) and in certain pathological conditions (such as Alzheimer's disease), it can be expressed by neurons (Hol et al., 2003). Other markers such as S100β, Aldh1L1, and Glt1 have also been used to identify astrocytes in the past.

1.3.1.3 Potassium Buffering Roles of Astrocytes

One important role of astrocytes is to maintain ion homeostasis in CNS tissue. Neurons rely on the concentration gradients of Na^+ (generally high extracellularly and low intracellularly), K^+ (generally low extracellularly and high intracellularly), and Cl^- (generally high extracellularly and low intracellularly) to generate graded and action potentials. When a neuron is depolarized in physiological conditions, sodium enters the cell and potassium exits the cell. If the depolarization reaches a certain threshold, the cell will fire an action potential. During sustained spike trains (several action potentials in a short period of time), a significant amount of potassium leaks out of the neuron, increasing the extracellular concentration of potassium. If extracellular potassium concentrations are too high, the neuron will fire action potentials repeatedly, which can result in seizure-like behavior. Astrocytes act as buffers of potassium. Astrocytes are also more permeable to potassium than neurons, due in part to high expression of inwardly rectifying potassium channels (K_{ir}) that are open at resting membrane potential. Active transport (via Na/K ATPase, the same one expressed by neurons) and cotransport (via Na^+-K^+-Cl^- cotransporter) mediate entry of potassium into the astrocyte (Kofuji and Newman, 2004). In this mode of potassium buffering, individual astrocytes take up excess K^+ and store it, releasing it back to the extracellular space when extracellular potassium concentrations have decreased. Naturally, water is drawn into astrocytes by potassium influx, resulting in cell swelling. The other type of extracellular potassium concentration regulation demonstrated by astrocytes is spatial buffering. In spatial buffering, potassium ions enter astrocytes and travel through the astrocyte syncytium (astrocytes can be coupled to one another via ion-permeable gap junctions) to a region where potassium efflux from astrocytes is favored. When there is a region of increased $[K^+]_o$, potassium ions are driven into astrocytes. This depolarization propagates to other astrocytes via gap junctions. In regions where $[K^+]_o$ is low, the driving force (V_m-E_K) causes K^+ to flow out of the cell.

This redistribution of extracellular potassium is dependent on the efficiency of coupling between astrocytes, unlike the net influx form of potassium buffering.

1.3.1.4 Role of Astrocytes in Glutamate Homeostasis

The role of the astrocyte is certainly not restricted only to ion buffering. Astrocytes also play a critical role in neurotransmitter uptake, particularly that of glutamate which can be excitotoxic at high concentrations. This is particularly important under circumstances of high frequency stimulation in which neurotransmitters can "spill over" from the synapse and activate extrasynaptic glutamate receptors. In some cases (but not all), extrasynaptic glutamate can be neurotoxic and it is associated with neurodegenerative diseases. For example, in ischemia, reduced cerebral blood flow leads to ATP depletion which in turn inhibits the Na^+/K^+ ATPase, thus inducing excessive depolarization of neurons and subsequent calcium toxicity (i.e. via activation of proteases and induction of apoptosis). Excessive calcium entry into neurons also feeds the cycle by promoting the release of the excitatory neurotransmitter glutamate. In normal conditions, astrocytes regulate extracellular glutamate concentrations by taking up glutamate via EAAT (EAAT/GLAST-1 and EAAT2/GLT). These proteins are transporters that mediate the influx of sodium, protons, and glutamate as well as the efflux of potassium. Relevant to the field of psychostimulant abuse, cocaine self-administration has been shown to downregulate GLT-1 expression and functional activity as well as system x_c^- expression and functional activity. Administration of the β-lactam antibiotic ceftriaxone restored expression of GLT-1 and attenuated cue- or cocaine-induced reinstatement of drug seeking behavior (Knackstedt et al., 2010). Inhibition of the Na^+/K^+ ATPase during ischemia causes the gradient used for cotransporting the molecule of glutamate to collapse and results in an inability of astrocytes to take up extracellular glutamate. The cystine-glutamate antiporter is also upregulated during ischemia, which contributes to glutamate release from astrocytes. Impaired glutamate homeostasis such as that observed in ischemia results in excitotoxicity at synaptic sites and extrasynaptic sites, resulting from increases in the calcium permeability of neurons, mediated primarily by the NMDA receptors. Activation of extrasynaptic NMDA receptors by glutamate overflow from astrocytes generates electrophysiological

events known as slow inward currents (SICs). These currents can be distinguished from sEPSCs by their much slower kinetics (both rise and decay kinetics) that can be modeled using a single exponential function during the decay phase. These SICs, despite being mediated primarily by extrasynaptic glutamate receptors (Pál, 2015), are essential for modulation of firing in the pendunculopontine nucleus (Kovács and Pál, 2017). Therefore, the notion that extrasynaptic glutamate activity is only associated with pathological conditions (i.e. apoptosis) is not universally true. These SICs are associated with many functions, including synchronization of neuronal circuits (Fellin et al., 2004).

Apart from the excitatory amino acid transporters, another transporter alters extracellular glutamate concentration. This transporter, known as system x_c^- mediates inward transport of cystine and outward transport of glutamate. Cystine is a necessary component of the antioxidant compound glutathione while glutamate is an excitatory amino acid neurotransmitter. System x_c^- is particularly enriched in glia, both microglia and astrocytes (Bridges et al., 2012). System x_c^- plays a role in relapse to cocaine seeking behavior: during withdrawal from a cocaine self-administration paradigm, extracellular glutamate levels decrease, in line with a decrease in the expression of x_c^-. Thus, transport by x_c^- decreases after withdrawal and restoring the function of x_c^- after withdrawal (using N-acetylcysteine, a cystine prodrug) can inhibit the reinstatement of cocaine-seeking behavior by a priming injection of cocaine. The increase in glutamate mediated by system x_c^- is thought to activate presynaptic group II metabotropic glutamate ($G_{i/o}$-coupled) receptors which decrease glutamate release and counter reinstatement behavior presumably by inhibiting glutamatergic afferents from the prefrontal cortex. Synaptic release of glutamate is associated with the reinstatement of drug-seeking behavior, and therefore stimulation of these metabotropic glutamate receptors by x_c^- decreases reinstatement of drug-seeking behavior (Baker et al., 2003). Transport by amino acid transporters is not the only proposed mechanism by which astrocytes regulate extracellular glutamate concentrations. Briefly, the gliotransmitter hypothesis posits that astrocytes can release neurotransmitters in response to stimuli from neurons. In the sections that follow, the gliotransmitter hypothesis will be discussed as a proposed mechanism by which astrocytes release glutamate. Moreover, astrocytes take up more than just glutamate. They also take

up GABA, adenosine (Boison et al., 2010), and glycine. Discussion of these other neurotransmitters is beyond the scope of this thesis, but there is a great amount of literature discussing these other neurotransmitters (Boison et al., 2010; Schousboe, 2003). Moreover, there are several excellent reviews summarizing glutamate homeostasis by astrocytes (Rose et al., 2017; Anderson and Swanson, 2000; Hertz et al., 1999; Kalivas, 2009).

1.3.1.5 Astrocyte Morphology

Astrocytes *in vivo* generally demonstrate a stellate morphology when stained with antibodies for glial fibrillary acidic protein (GFAP), a common marker for astrocytes (Figure 1.2). The cell body of the astrocyte is generally quite small and the majority of the astrocyte surface area is made up of long ramifications on which there are a large number of finer processes. These long ramifications are typically visible in brain tissue immunostained for GFAP. However, GFAP is expressed heterogeneously among astrocytes, and moreover, is not found in the fine processes of astrocytes (Verkhratsky and Nedergaard, 2018). This constitutes a critical limitation of utilizing GFAP as a marker to visualize astrocytes; up to 95% of the volume contained by an astrocyte is localized in the peripheral processes (Shigetomi et al., 2013). Thousands of these extremely fine astrocytic processes therefore contribute to the bulk of the volume of astrocytes. Several approaches have been employed to view the finer processes of astrocytes that form the perisynaptic and endfoot domains of the astrocytes including iontophoresis with Lucifer Yellow (Moye et al., 2019) and genetically encoded fluorescent proteins targeted to the plasma membrane rather than the cytosol (Testen et al., 2020). These approaches reveal a "cloud" of fine astrocytic processes that extend from the main processes of astrocytes. Such processes contain calcium microdomains that are highly relevant to studies of astrocyte physiology (Shigetomi et al., 2013). Many of these fine processes are often called perisynaptic astrocytic processes (PAPs) due to their extremely close proximity to the postsynaptic density and the presynaptic terminals of neurons.

A key distinction between astrocytes *in vivo* and astrocytes in monoculture is that astrocytes in culture do not normally possess the same stellate morphology. Astrocytes in

culture are generally flat and polygonal (Figure 1.3). They can be induced to take on a stellate morphology by adding cAMP to the culture media, but this process of stellation does not resemble that which occurs during development (Schiweck et al., 2018). Astrocytes in culture also take on a more stellate morphology in the presence of dopamine (Galloway et al., 2018), possibly via cAMP synthesis induced by D_1 receptor activation. It is possible to replicate the morphology seen *in vivo* in culture, complete with fine processes that possess calcium transients. This can be achieved by co-culture with neurons with added heparin-binding epidermal growth factor or in cultures containing heparin-binding epidermal growth factor (HBEGF) and neurobasal medium (media derived from a culture of neurons); These astrocytes demonstrated stellate morphology (Wolfes et al., 2017). Moreover, when media is supplemented with HBEGF, astrocytes demonstrate calcium transients (Morita et al., 2003).

Like their microglial counterparts, astrocytes can enter a "reactive" state characterized by several phenotypic characteristics. This "reactive" state is just as nebulous as it is in microglia (in which reactive microglia were previously classified as M1 or M2), and classification of single cells beyond reactive and non-reactive may not be possible without rigorous transcriptomic analysis, however, at least one review posits two distinct phenotypes of reactive astrocytes (Liddelow and Barres, 2017). The protein GFAP has long been utilized as a marker indicating astrocyte reactivity. Part of the reason for why GFAP has been utilized as a marker for reactivity is that astrocytes were thought to be highly proliferative in the reactive state and indeed in some pathological states, there is dramatic upregulation of GFAP. In fact, astrocytes do not exhibit such extreme proliferative activity, and there is only a modest increase in proliferation after severe physical injury (i.e. a stab wound). Paralleling the classification of reactive microglia, an A1 and A2 type of reactive astrocyte have been proposed. The A1 astrocytes typically express pro-inflammatory molecules such as TNFα and IL-1β while the A2 astrocytes are immunosuppressant and express genes such as *Arg1* and *Fzd1*. Ischemia in particular induces polarization to the A2 state in which neurotrophic factors are synthesized while inflammatory insults induce polarization to the A1 state. Therefore, the A2 state parallels the M2 state of microglia (by serving reparative functions) while the A1 state parallels the M1 state of microglia (by

serving inflammatory functions). In reality, this polarization may be an extreme oversimplification; The M1/M2 polarization of microglia has been called into question, and thus, it is plausible that the A1/A2 polarization of astrocytes may also be problematic (Ransohoff, 2016). Thus, just as in microglia, the fate of the A1/A2 argument will rely on results from single-cell RNASeq (transcriptomic) analyses.
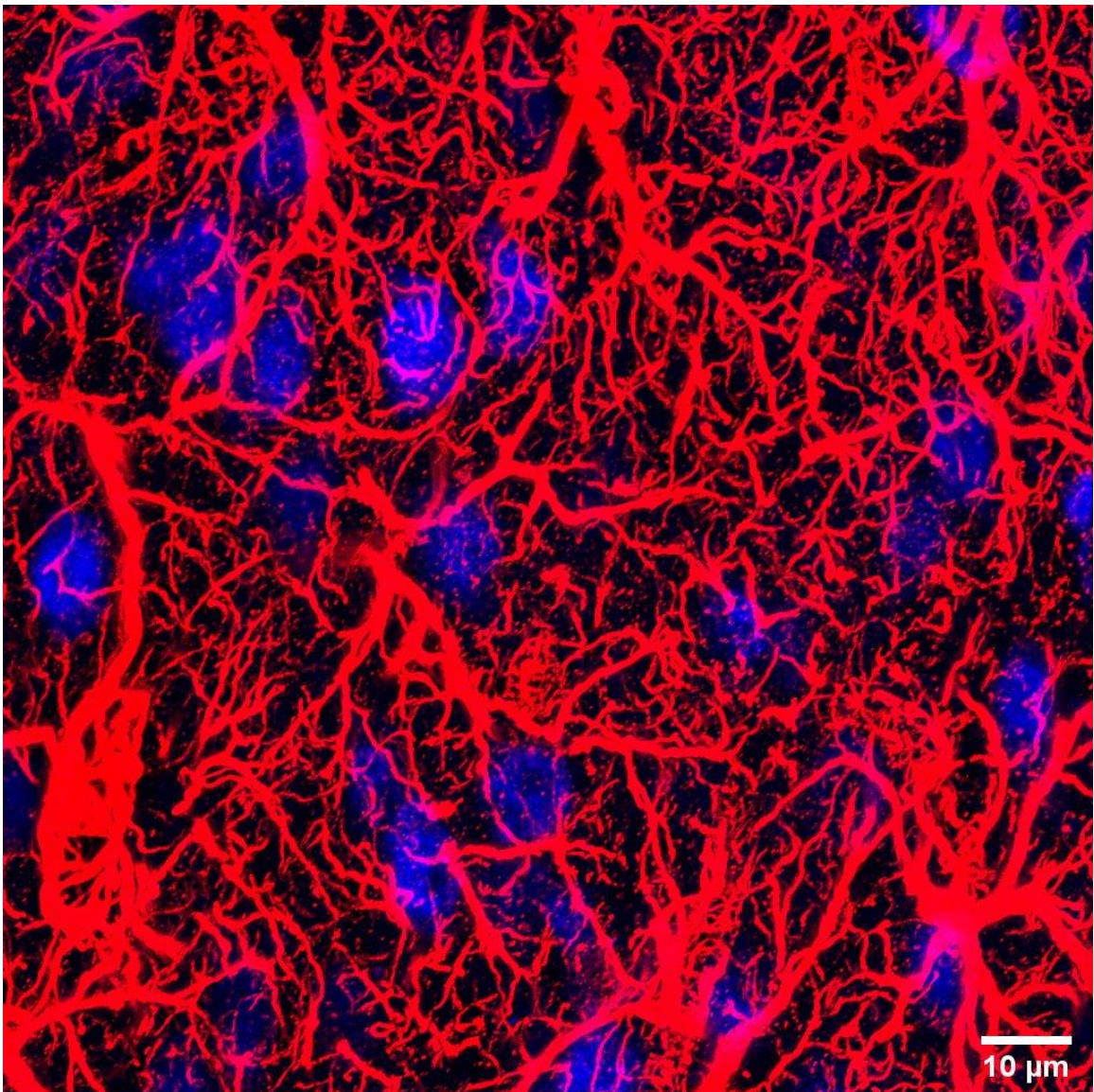
Figure 1.2 A max intensity projection of rat prefrontal cortex tissue stained for GFAP (*red*), an astrocytic marker and NeuN (*blue*), a neuronal marker, viewed with a confocal microscope. Astrocytes demonstrate a stellate morphology *in vivo*. Note that only a fraction of astrocytes in the field are stained with anti-GFAP antibody. Image taken by Richik Neogi.
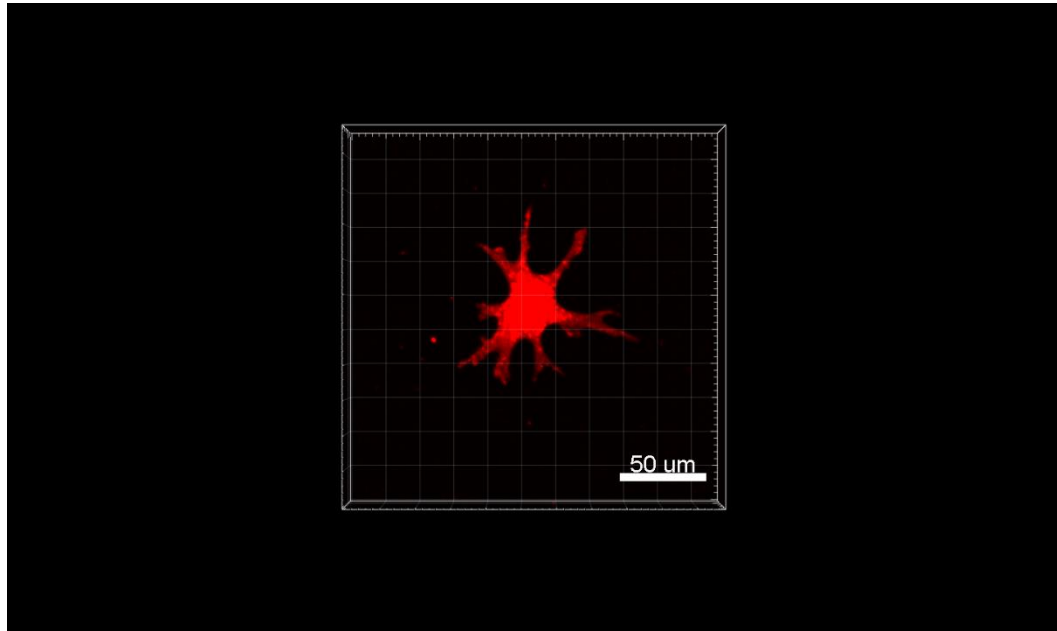
Figure 1.3 Astrocytes in culture take on a distinct polygonal morphology. Here tdTomato was expressed under the GFAP promoter (image taken by Surya Aryal, reproduced with permission)

1.3.2 Astrocytic Calcium

Calcium is a unique ion in living systems in that it is also a second messenger. While other ions like sodium and potassium exert their effects on a cell primarily via an electrochemical gradient, calcium acts as a direct transducer of cell signaling. Intracellular calcium concentration varies spatially and temporally in a typical living cell; analysis of such calcium transients has become a field in and of itself. Initial studies of astrocytic calcium transients involved bulk loading calcium-sensitive, membrane permeable dyes or patch dialysis of calcium-sensitive dyes (Russell, 2011). These approaches do not allow for visualization of the entire astrocyte and come with their own problems that limit their use when analyzing physiologically relevant intracellular calcium signaling. The

introduction of genetically encoded calcium indicators (GECI) revolutionized the field of astrocyte physiology because these indicators can be expressed throughout the astrocyte in different compartments (plasma membrane, cytoplasm, endoplasmic reticulum) which allows for visualization of calcium activity in fine astrocytic processes (Tong et al., 2012). Introduction of a GECI to a live animal entails surgery and injection of a viral vector carrying the GECI gene alongside a promoter (GFAP and GfABC$_1$D are two documented promoters for successful expression in astrocytes) directly into brain parenchyma. Since the GECI itself is fluorescent, there is no need to employ a reporter to indicate successful transfection. This technique is extraordinarily useful because it not only allows for imaging in brain slices, but also *in vivo* imaging. The Lck-GCaMP3 transgene targets the GECI GCaMP3 specifically to the plasma membrane. Using an AAV2/5 vector, Shigetomi and coworkers (Shigetomi et al., 2013) successfully achieved hippocampal expression of Lck-GCaMP3 and cyto-GCaMP3. The Lck-GCaMP3 animals, in particular, revealed the presence of calcium microdomains in the fine astrocytic processes that previously could not be effectively visualized. The Lck-GCaMP3 animals expressed GCaMP3 in a "cloud" surrounding the astrocyte soma whereas the cyto-GCaMP3 animals expressed GCaMP3 in a more traditional fashion (similar but not identical to that revealed by GFAP IHC). Both were expressed in the entire astrocytic territory. Analysis of calcium activity using GECIs and the calcium indicator Fluo-4AM revealed that the GECIs revealed a greater number of calcium events than the organic calcium indicator.

Calcium transients in astrocytes are not simply epiphenomena of astrocyte physiology; they play a direct role in brain function. The gliotransmitter hypothesis posits that astrocytes can release substances that can influence neurotransmission; this hypothesis will be the subject of the next section. Another function of calcium in astrocytes is to promote vasodilation of cerebral vasculature via activation of the calcium-dependent phospholipase A$_2$ (cPLA$_2$) which releases arachidonic acid from membranes. This arachidonic acid is processed to prostaglandins by cyclooxygenase. Prostaglandins dilate vasculature. It was demonstrated that stimulation of G$_q$-coupled metabotropic glutamate receptors releases prostaglandin and is also associated with vasodilation (Zonta et al., 2003), although there is some evidence that astrocytic calcium signaling induced by G$_q$ is

too slow to account for stimulus-induced vasodilation and that mice lacking the gene for the major inositol triphosphate receptor mediating calcium release from the ER (IP$_3$R2) still exhibit stimulus-induced vasodilation (Nizar et al., 2013).

In astrocytes, calcium can enter the cytosol from three different compartments. It can enter through the plasma membrane by calcium channels driven by the electrochemical gradient between the cytosol and the extracellular fluid, it can enter by release from the endoplasmic reticulum via inositol triphosphate (IP3R) or ryanodine receptors (RyR), or it can be released from the mitochondria, particularly when the cell is apoptotic. A fourth form of calcium entry can be mediated by connections with other astrocytes (through gap junctions).

Astrocytes express a variety of calcium channels. In addition to channels such as Orai, which serve to replenish intracellular (endoplasmic reticulum) stores of calcium, astrocytes also express voltage-gated calcium channels (VGCCs). Voltage-gated calcium channels can be divided into four classes based on electrophysiological and pharmacological properties. The L-type calcium channel has been proposed to promote the "reactive" state of astrocytes, and indeed LPS-induced reactivity is associated with a proportionate increase in Ca$_v$1.2 expression (Cheli et al., 2016). However, the distribution of VGCCs in astrocytes is not uniform across all brain regions. Ligand-gated calcium channels such as the P2X receptors also can plausibly mediate calcium entry into astrocytes. The P2X7 receptor, activated by high concentrations of ATP, can mediate pro-inflammatory functions of astrocytes (Panenka et al., 2001) and moreover, activation of glial P2X7 receptors can modulate synaptic activity in the hippocampus (Khan et al., 2019). The subject of ion channels on astrocytes has been reviewed in detail elsewhere (Verkhratsky and Steinhäuser, 2000). The form of calcium entry that has been supported by the largest amount of evidence, however, is that mediated by release from the endoplasmic reticulum.

Activation of G$_q$ coupled GPCRs initiates an intracellular cascade that results in the release of inositol triphosphate (IP$_3$) and diacylglycerol (DAG) from

phospholipids at the plasma membrane via the action of phospholipase Cβ. The second messenger IP_3 then activates IP_3 receptors (IP_3Rs) located in the membrane of the endoplasmic reticulum, resulting in the release of calcium from intracellular stores. Activation of a wide variety of G_q coupled receptors can initiate calcium activity in astrocytes including glutamate (Sun et al., 2013), $GABA_B$ (Mariotti et al., 2016), dopamine D1 (Liu et al., 2009), and P2Y (Gallagher and Salter, 2003) receptors. Depending on spatial and temporal localization, ligands for these receptors can have differential effects on calcium transients. For example, the P2Y2 receptor promotes more rapidly traveling calcium waves than the P2Y1 receptor, however the nucleotidase apyrase blocks the calcium waves produced by P2Y2 receptor activation, but enhances those produced by P2Y1 receptor activation (Gallagher and Salter, 2003). The specific isoform of the IP_3R that is associated with calcium transients in astrocytes has been proposed to be IP_3R2 (Petravicz et al., 2014). Experiments by this group in which IP_3R2 was knocked out suggested that G_q-mediated calcium signaling was abolished. Indeed, knockout mice (IP3R2 -/-) survive to maturity and there was a significant reduction in the frequency, amplitude, and duration of somatic calcium transients (Srinivasan et al., 2015). However, there was a much less pronounced effect in the processes of astrocytes, which constitute the bulk of the volume contained by astrocytes. The frequency of calcium transients was not significantly reduced. The duration of calcium transients in the processes was increased in IP_3R2 (-/-) mice and the amplitude was significantly decreased. Knockout of IP_3R2 did not decrease the mean fluorescence of averaged traces compared to WT mice. The contribution of transmembrane calcium flux was quantitated using calcium-free buffer – it was found that calcium-free buffer abolished calcium waves and reduced the basal intensity of calcium signals. It is therefore plausible that transmembrane flux of calcium plays a role in calcium transients, perhaps those mediated by the TRPA1 channel (Shigetomi et al., 2011).

However, IP_3R2 knockout could not abolish calcium transients in the peripheral processes evoked by endothelin, a ligand for a G_q-coupled receptor. It was observed that only somatic calcium fluctuations mediated by the endothelin receptor could be abolished. In live unanesthetized animals, it was observed that the frequency of calcium events in

microdomains (located in the processes of astrocytes primarily) was slightly but significantly reduced, the amplitude was *increased*, and the duration of these calcium events was unaffected by IP$_3$R2 knockout (Srinivasan et al., 2015).

Thus, there is robust evidence that intracellular calcium transients occur in astrocytes, even with astrocytes in physiological conditions. Both GECIs and calcium-sensitive dyes can detect these calcium transients, but GECIs do so more effectively because they reach all parts of the astrocytes, including the fine processes. The precise function of these transients in the cell is currently unknown; whether these calcium transients are responsible for the release of gliotransmitters is a matter of debate in the field, with one camp insisting that gliotransmitter release occurs *in vivo* (Savtchouk and Volterra, 2018) and the other insisting that it does not occur in physiological conditions (Fiacco and McCarthy, 2018).

CHAPTER 2. THE SIGMA-1 RECEPTOR

2.1 Molecular Biology and History of the Sigma-1 Receptor

The sigma receptors were initially characterized as novel subtypes of the opioid receptor family based on studies that revealed the existence of multiple subtypes of opioid receptors in the spinal dog (Martin et al., 1976). In these studies, morphine was characterized as the prototypical μ-opioid receptor agonist, ketocyclazocine as the prototypical κ-opioid agonist, and the benzomorphan SKF-10,047 as the prototypical σ-receptor agonist. It was later determined that SKF-10,047 binds to sites in the guinea pig brain that are not accessible to the potent opioid ligand etorphine, and that this binding could not be occluded by the opioid antagonist naltrexone (Su, 1982). Thus, the "σ-opioid receptor" was renamed the σ-receptor (Su et al., 1988).

The sigma-1 receptor (herein referred to as the S1R) was first successfully cloned in 1996 (Hanner et al., 1996). The corresponding mammalian open reading frame encodes a protein of mass 25.3 kDa with at least one transmembrane segment. The primary structure of the protein contains a putative endoplasmic reticulum retention signal (WAVG**RR**), and shares sequence homology (67% sequence homology) with a fungal C8-C7 sterol isomerase, but does not share sequence homology with any other known mammalian protein (Moebius et al., 1997).

The structure of the S1R has been the subject of debate since its discovery. Computational algorithms predict the presence of two to three transmembrane domains (Bolshakova et al., 2016), and some experimental evidence suggests the presence of two transmembrane domains (Aydar et al., 2002; Mori et al., 2013). In the study by Aydar and coworkers, GFP was fused either to the C-terminus or the N-terminus. In *Xenopus* oocytes, the fluorescence was localized towards the cytoplasmic face of the plasma membrane for both constructs. This suggests the existence of an even number (i.e. two) of transmembrane segments, as the constructs would differ in terms of fluorescence localization if there were an odd number of transmembrane segments. Nevertheless, the x-ray crystallographic structure of the human S1R reveals an assembly of three protomers, each with a single

transmembrane domain; this directly contradicts the findings suggesting two transmembrane domains (Schmidt et al., 2016).

2.2 Sigma-1 Receptor Ligands

The S1R is a unique receptor in that its mode of signal transduction does not rely on commonly known signal transduction cascades (i.e. those mediated by G-proteins or receptor tyrosine kinases). Rather, its "activity" is characterized by association with various partner proteins upon binding of a ligand. This has led to the classification of the S1R as a "ligand-regulated non-ATP binding membrane-bound chaperone protein (Chu and Ruoho, 2016)." Moreover, ligands for the sigma-1 receptor are structurally diverse (Figure 1.1 and Figure 1.2)

Helices in the C-terminal region of the S1R are responsible for interaction with binding immunoglobulin protein (BiP), and it is thought that binding of ligand to the receptor alters the ability of the S1R to form oligomers (Gromek et al., 2014) via a GXXXG motif at the C-terminus. Before addressing whether certain ligands are agonists, antagonists, or inverse agonists, it is important to determine the structural requirements for a compound to be a ligand of the S1R.

A triple-mutant S1R with alanine substitutions at L105, L106, and S93 demonstrated markedly reduced binding to NE-100 as did a mutant with a phenylalanine substitution at Y103 and an alanine substitution at S93 also demonstrated similarly reduced binding. Interestingly, the triple-mutant S1R did not demonstrate reduced affinity for the S1R agonist (+)-pentazocine (Yamamoto et al., 1999), suggesting differences in the binding requirements for agonists (pentazocine) and antagonists (NE-100).

With the exception of the cholesterol-based ligands of the S1R (which bind to a distinct site separate from other ligands), all known S1R ligands possess a basic nitrogen atom that is critical for interaction with the S1R. Removal of the nitrogen atom from phenalkylpiperidine derivatives abolished S1R binding (Ablordeppey et al., 2000). Indeed,

29

the presence of a basic nitrogen atom flanked by two longer hydrophobic moieties has been termed the minimal S1R-binding pharmacophore (Schmidt et al., 2018). The notion that a basic nitrogen atom is critical for ligand binding was confirmed when cells treated with the crosslinking reagent 1-ethyl-3-(3-dimethylaminopropyl)carbodiimide (EDC) expressed dramatically reduced affinity for radiolabeled haloperidol and radiolabeled pentazocine. In this context, crosslinking reagents are those that facilitate peptide bond formation between a sidechain carboxyl group and a free amino group. These findings were corroborated by the observation that the S1R mutants D126G and E172G demonstrated only 9% and 3% of the binding to [^{3}H]haloperidol relative to the wild-type control (Seth et al., 2001). In fact, both agonists and antagonists of S1R require the presence of E172, as revealed by an x-ray crystallography study assessing the pose and interactions with the S1R of NE-100, haloperidol, and (+)-pentazocine (Schmidt et al., 2018). However, antagonists and agonists differ in terms of their binding to other regions of the S1R. Per the minimal S1R-binding pharmacophore, antagonists take on a linear pose in the binding site with the primary (longer) hydrophobic arm pointed between α-helix 4 (α4) and α-helix 5 (α5). The shorter hydrophobic arm of the antagonist occupies the space near D126. In contrast, for the agonist (+)-pentazocine (and likely for all S1R agonists containing a basic nitrogen), binding forces α4 away from α5. Moreover, S1R agonists generally have a nonlinear structure. Thus, in the antagonist-bound state, α4 adopts a similar position to that of the ligand-free S1R. In the agonist-bound state, S1R must undergo a conformational change to prevent steric clash with the ligand. The authors verified that other agonists bind in this manner by docking PRE-084 to S1R, indicating that this conformational change is required for broader efficacy of all S1R agonists. In kinetic experiments measuring the on and off rate of (+)-pentazocine and haloperidol, it was determined that there was a rate-limiting step that was ligand-independent, meaning that for binding to occur, S1R must adopt a proper conformation. Through MD simulation experiments, it was found that binding pathway requires two conformational changes in the structure of S1R, independent of the ligand. These states were reversible, suggesting that binding is stochastic; in order for an agonist to bind, the receptor must occupy a certain conformational state.

The S-(+) isomer of methamphetamine is a ligand at the S1R with an affinity comparable to that of cocaine (2 µM in the mouse brain in competition with pentazocine for cocaine and 2.16 µM in the rat brain in competition with pentazocine for methamphetamine). There is conflicting data regarding whether methamphetamine is an agonist or an inverse agonist at the sigma-1 receptors. Agonists of the S1R normally induce dissociation of S1R from binding of immunoglobulin (BiP). Methamphetamine increased the association of BiP with S1R, as demonstrated by co-immunoprecipitation experiments, although this finding failed to reach significance ($p > 0.05$) while (+)-pentazocine and PRE-084 significantly induced dissociation of BiP from S1R (Hayashi and Su, 2007). Interestingly, cocaine did not significantly alter the association of S1R with BiP either, suggesting that this assay may not be able to unambiguously distinguish weak agonists from antagonists. Thus, the identity of various ligands as agonists or antagonists is still up for debate, as these results clearly show that some agonists do not dissociate S1R from BiP while others do. The previously cited affinities of methamphetamine and cocaine for the S1R are near to those reached in physiologically relevant cocaine or methamphetamine administration paradigms (Yasui and Su, 2016). Many of the behavioral effects of cocaine (i.e. cocaine-induced CPP) are attenuated by administration of S1R antagonists such as NE-100 and BD-1047 (Romieu et al., 2001). Similarly, administration of MS-377, a S1R antagonist, attenuates the development of locomotor sensitization to methamphetamine (Takahashi et al., 2000). There is however, some conflicting data on whether it is an agonist or an inverse agonist for S1R based on cellular data. Methamphetamine behaves as a an S1R agonist behaviorally while there is conflicting evidence for its actions at the S1R receptor at a molecular and cellular level.
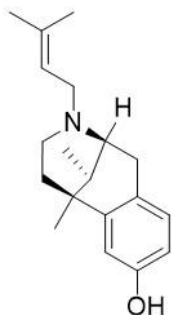
(+)-Pentazocine
K_i = 0.0012 µM
guinea pig brain
Hellewell & Bowen, 1990
agonist
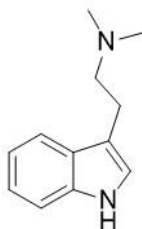
N,N-dimethyltryptamine
K_D = 14.75 µM
guinea pig/rat liver
Fontanilla et al., 2009
agonist
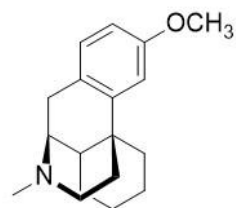
Dextromethorphan
K_i = 0.403 µM
rat brain homogenate
Fishback et al., 2012
agonist (Nguyen et al., 2014)
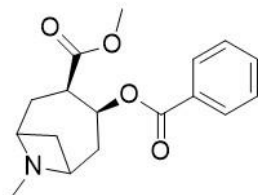
Cocaine
K_i = 2 µM
mouse brain
Matsumoto et al., 2002
agonist
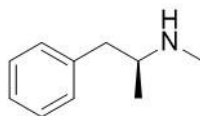
(S)-(+)-methamphetamine
K_i = 2.16 µM
rat brain
Nguyen et al., 2005
unknown whether agonist or
inverse agonist
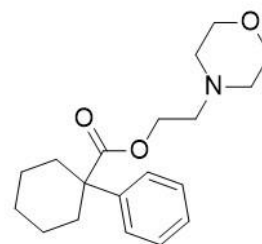
PRE-084
IC50 = 0.188 µM
mouse brain
Entrena et al., 2016
agonist

Figure 2.1 Sigma-1 receptor agonists are structurally diverse; most possess nonlinear
structures
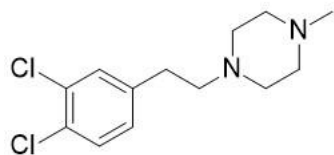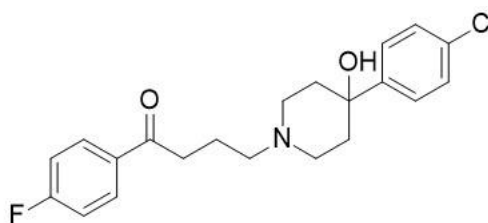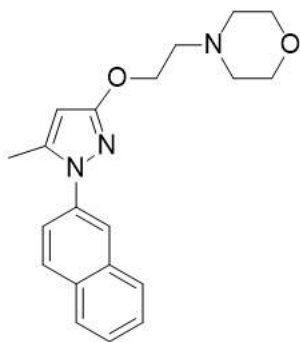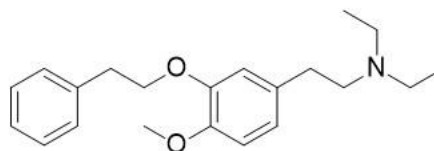
Figure 2.2 Sigma-1 receptor antagonists possess a more linear structure than agonists

2.3 Sigma-1 Receptor and DA Signaling

Given that two major psychostimulants (METH and cocaine) are both ligands of the S1R, one can speculate that the effects at the S1R could alter dopamine receptor signaling or uptake of dopamine by DAT since the S1R is known to interact with GPCRs (Kim et al., 2010) and many other client proteins. Indeed, BRET experiments in HEK293T cells suggest that S1R forms a heteromer with the D1 dopamine receptor and the agonist-

bound form of S1R stabilizes the outward-facing conformation of dDAT, enhancing binding of cocaine in the process (Hong et al., 2017).

That the S1R interacts with DAT is particularly relevant to mechanisms of psychostimulant action, since two major psychostimulants, cocaine and methamphetamine, are ligands of the S1R as well as DAT. In rat brain tissue, the sigma-1 receptor agonists PRE-084 and (+)-pentazocine increased the B_{max} of [^{3}H]WIN35428 (a DAT inhibitor) without altering K_i and both drugs also increased the V_{max} of dopamine transport by DAT in low sodium conditions (conditions unfavorable towards inward transport by DAT). It was also shown in HEK293 cells transfected with dDAT that S1R forms a heteromer with DAT, much like the S1R does with D1 receptors. When proteins change conformation, sometimes cysteine residues become exposed to the extracellular milieu. It is possible to manipulate this change in accessibility using a cysteine accessibility assay. In this assay, when a drug is added, the conformation of the protein changes in a way that exposes cysteine residues to a thiol-reactive reagent. It was found that PRE-084, only in the presence of cocaine, increased C306 accessibility. This increase was abolished by treatment with a selective S1R antagonist (Hong et al., 2017). This study also recapitulated the idea that S1R forms higher order oligomers upon treatment with antagonists and can only interact with DAT in the form of lower order S1R oligomers (dimers and monomers).

Some studies suggest that activation of the sigma-1 receptor during exposure to methamphetamine opposes the behavioral and cellular effects of METH such as locomotor sensitization and METH-mediated dopamine efflux. Treatment with PRE-084, a S1R agonist, or upregulation of the S1R during exposure to methamphetamine in the bath inhibits METH-stimulated firing activity in dopaminergic neurons. Moreover, treatment with 1 μM PRE-084 decreased METH-mediated dopamine efflux *in vivo* and *in vitro* while BD1063 had no effect. The study found that S1R colocalizes with DAT at the plasma membrane, and its association with DAT is increased when METH is present in the bath (Sambo et al., 2017). That S1R is found to be localized at the plasma membrane associated with DAT and that METH alone produced no change in the localization provides an argument against the assumption that METH is an inverse agonist at S1R, since an inverse

agonist would increase the number of higher-order (DAT unassociated) oligomers which in turn would localize at the ER. Some studies have suggested that intracellular calcium is necessary for dopamine efflux induced by AMP via DAT as well as inward currents mediated by AMP (Gnegy et al., 2004). Indeed, AMP can increase $[Ca^{2+}]_i$ in a DAT-dependent manner. This increase in intracellular calcium could be blocked by depleting calcium in the ER using thapsigargin, suggesting that the increase in calcium is not due to transmembrane flux, but rather due to release from the ER, although there is evidence to suggest that the increase in intracellular calcium was only observed in the presence of extracellular calcium (Mundorf et al., 1999). In the work by Sambo and coworkers, neurons either expressing GCaMP6f or loaded with Fura-2-AM were assessed for calcium activity in the presence of METH and/or PRE-084. It was observed that METH alone increased intracellular calcium and this increase could be blocked by the DAT inhibitor nomifensine. This increase could also be blocked by the S1R agonist PRE-084. This study also revealed that PRE-084 attenuated behavioral responses (ICSS, CPP, and locomotor activity) to methamphetamine administered by the experimenter (Sambo et al., 2017), although the S1R antagonist BD-1063 also attenuated these responses. Interestingly, a previous study examining the effects of S1R agonists on methamphetamine-induced behavior found that the S1R agonist SA4503 attenuated radiolabeled dopamine efflux, yet it potentiated some behaviors associated with methamphetamine such as those during drug-discriminatory tasks and also attenuated others such as locomotor activation. However, S1R antagonists BD1047 and BD1063 had no effect on radiolabeled dopamine efflux (Rodvelt et al., 2011).

The S1R forms oligomers with several GPCRs such as the mu-opioid receptor (Kim et al., 2010) and modulates the activity of the GPCR. It has been demonstrated that the D1 dopamine receptor also interacts with S1R and S1R interaction with D1R can modulate the activity of the D1R. Agonists at the S1R can enhance PKA activation in rat synaptosomal preparation (from the prelimbic cortex) through the D1R in the presence of a selective D1R agonist. This effect was clearly mediated by the S1R because it was abolished by incubation with a S1R antagonist. The S1R agonist enhanced PKA activation in the presence of a cell-permeable cAMP analog and in the presence of forskolin, an adenylyl cyclase activator, but did not enhance adenylyl cyclase stimulation by G_s in the presence

of a dopamine D1 receptor agonist. This suggests that S1R could act somewhere downstream of the receptor itself to enhance PKA activation. This increase in PKA activation by S1R agonist could be blocked by incubation with the PKC inhibitor chelerythrine as well as incubation of synaptosomes in EGTA-containing buffer, suggesting that PKC and calcium mediate the effect on PKA activation. Moreover, blockade of voltage-gated calcium channels also abolished the effect of S1R agonist on PKA activation, suggesting that the source of this calcium is transmembrane flux. It was demonstrated that PKC is upstream of the increase in intrasynaptosomal calcium, and that chelerythrine abolished the increase in calcium concentration. Incubation with the ER calcium-depleting agent thapsigargin had no effect on the increase in intrasynaptosomal calcium mediated by S1R activation (Fu et al., 2010). Interestingly, PKC in astrocytes has been implicated in mediating long-lasting behavioral sensitization induced by methamphetamine. Moreover, incubation of cultures with 10 µM methamphetamine (within the range considered "physiological") increased stellation that could be partially abolished by treatment with a PKC inhibitor. Similarly, incubation with this concentration of methamphetamine also increased GFAP immunoreactivity and intracellular calcium activity evoked by 10 µM of dopamine and glutamate (Narita et al., 2005).

To investigate the effects of the S1R-D_1 receptor action in cocaine administration, Navarro and colleagues utilized a variety of techniques to demonstrate the existence of a D_1-S1R heterooligomer and assessed cocaine's effects on this oligomer (Navarro et al., 2010). In HEK293T cells, BRET (between σ_1-YFP and D_1-Rluc) was utilized to determine the existence of heterooligomers and indeed it was determined that a heterooligomer between the S1R and D_1 receptor exists in cell culture. Moreover, treatment with cocaine induced translocation of S1R to the plasma membrane and colocalization with the D_1 receptor. Utilizing a D_1-YFP and D_1-Rluc pair, the BRET signal was reduced dose-dependently in the presence of cocaine, suggesting that S1R receptor activation disrupts D_1 receptor homodimers. In CHO cells, cocaine robustly enhanced cAMP accumulation induced by treatment with a selective D_1 receptor agonist. When CHO cells were treated with cocaine alone, there was no increase in cAMP accumulation, however, when they were treated with cocaine and SKF-81297, a D_1 receptor agonist, there was potentiation of

cAMP accumulation. Similarly, D_1 receptor-mediated phosphorylation of ERK1/2 by activation via SKF-81297 could be blocked by administration of PD-144,418, an S1R antagonist. Cocaine and PRE-084 could increase the phosphorylation of ERK1/2 in the absence of a D_1 receptor ligand. However, in combination with a D_1 receptor agonist (SKF-81297), cocaine and PRE-084 counteracted the increase in ERK1/2 phosphorylation by SKF-81297. The results from the cAMP accumulation and ERK1/2 phosphorylation experiments were recapitulated in slices from mouse striatum; incubation with either the D_1 receptor agonist or cocaine increased phosphorylation of ERK1/2. Moreover, in striatal slices from S1R knockout animals, cocaine was unable to induce ERK1/2 phosphorylation. Therefore, when present in this heterooligomeric form with the D_1 receptor, the sigma-1 receptor can phosphorylate ERK1/2 alone, but when both a sigma-1 receptor agonist and a D_1 receptor agonist are present, ERK1/2 phosphorylation is counteracted, suggesting an antagonistic interaction between the two receptors. A potential area of further research would be to observe if these findings can be recapitulated in pure astrocyte culture or astrocyte-rich cell culture.

The S1R also forms complexes with the dopamine D2 receptor, however in this case, the S1R turns down signaling via the D2 receptor (Navarro et al., 2013). Like in the previous report regarding D_1 receptors, $D_2/D_3/D_4$ receptors were fused to Rluc and σ_1 receptors to YFP. A significant BRET signal was observed with D_2 receptors but not with D_3 or D_4 receptors in HEK293T cells. Moreover, after transfection with D_2 receptor cDNA, colocalization between S1R and D_2 receptors was detected. In cells expressing both Rluc-S1R and YFP-S1R, homodimers between S1R protomers were detected via BRET and heterooligomers of S1R with D_2 receptor homodimers were detected as well. Diheterotetramers (S1R-S1R-D_2-D_2) were detected using a modified BRET protocol. Further BRET experiments revealed that activation of the S1R induces changes in the D_2-D_2 homomers and in the S1R-D_2 heteromers. In functional assays using CHO cells, it was determined that cocaine alone does not elicit any changes in D_2 receptor signaling, but there is a small but significant decrease in D_2 receptor signaling when cells were pretreated with cocaine (30 µM) and then treated with increasing concentrations of quinpirole. Moreover, cocaine significantly decreased the D_2-mediated decrease in forskolin-

stimulated cellular cAMP evoked by the D_2 receptor agonist quinpirole. This effect was also observed when PRE-084 was utilized in lieu of cocaine. However, when both quinpirole and cocaine were incubated with cells at the same time, negative cross-talk was detected, indicating an antagonistic interaction between the two receptors. It was also determined that activation of the S1R in the D_2-S1R heteromer can induce phosphorylation of ERK1/2 and that the D_2 antagonist raclopride or S1R antagonist PD144418 could inhibit ERK1/2 phosphorylation. To investigate whether these results could be recapitulated in mouse striatum, first, a Western blot and coimmunoprecipitation experiment were conducted. It was found that S1R was detected in WT but not S1R KO mouse striatum and D_2 receptors were expressed in both groups. The coimmunoprecipitation experiments revealed that the S1R does indeed form stable oligomers with the D_2 receptor. A proximity ligation assay also confirmed that the S1R formed stable oligomers with the D_2 receptor and that these results were not artifacts of detergent solubilization. Moreover, the antagonistic interaction on ERK1/2 phosphorylation was also observed in mouse striatal tissue: incubation with both quinpirole and cocaine abolished ERK1/2 phosphorylation, but when incubated with either compound alone, an increase in ERK1/2 phosphorylation was observed.

Thus, the sigma-1 receptor interacts directly with both the D_1 and D_2 receptors. It has also been suggested that the sigma-2 receptor interacts with the D_1 receptor but not the D_2 receptor. While the sigma-2 receptor is beyond the scope of this chapter, it is important to note that it does interact with the D_1 receptor exclusively. Evidence suggests that the sigma-1 receptor may form a heterotrimeric complex with the sigma-2 and D_1 receptors. When siRNA for the sigma-1 receptor was introduced to HEK293T cell culture (thus disrupting the heterotrimeric complex), cocaine and an agonist for the sigma-2 receptor reduced cAMP formation in the presence of a D_1 receptor agonist. Conversely, when siRNA for the sigma-2 receptor was introduced, cocaine potentiated agonist-induced cAMP formation. In cells lacking the sigma-1 receptor, but expressing D_1 receptor and sigma-2 receptor, cocaine pretreatment potentiated ERK1/2 phosphorylation via a D_1 receptor agonist. In cells that expressed the sigma-1 receptor and D_1 receptor but not the sigma-2 receptor, cocaine inhibited ERK1/2 phosphorylation via a D_1 receptor agonist.

Moreover, when all three receptors (sigma-1, sigma-2, and D_1) were expressed in cell culture, there was no effect of cocaine on cAMP accumulation or ERK1/2 phosphorylation, suggesting an antagonistic interaction between the sigma-1 receptor and sigma-2 receptor on the D_1 receptor. In striatal sections from rats injected acutely or chronically with cocaine, differences were observed in terms of the number of cells expressing D_1-σ_1 oligomers or D_1-σ_2 oligomers. For cocaine-naïve animals, 38.5% of cells expressed D_1-σ_1 oligomers and 25% of cells expressed D_1-σ_2 oligomers. In animals acutely treated with cocaine, the number of both oligomeric complexes (measured by counting puncta) was increased, but 54% of cells expressed D_1-σ_1 oligomers and 33% expressed D_1-σ_2 oligomers. When animals were treated chronically with cocaine, the number of D_1-σ_1 oligomeric complexes and the number of cells expressing D_1-σ_1 oligomers were restored to that of cocaine-naïve animals, but the number of D_1-σ_2 oligomeric complexes remained elevated and the number of cells expressing D_1-σ_2 complexes remained approximately the same. These results suggest that acute administration of cocaine drives increases in primarily the D_1-σ_1 oligomers, but chronic administration of cocaine drives an increase in D_1-σ_2 receptor oligomers (Aguinaga et al., 2018).

2.4 Physiology of the Sigma-1 Receptor

2.4.1 Sigma-1 Receptor Localization

The sigma-1 receptor is primarily an ER-localized protein. In particular, it is enriched at the mitochondrial associated membrane (MAM), the junction between mitochondria and the ER, where it can regulate calcium flux into mitochondria by associating with IP_3 receptors. It forms raft-like microdomains enriched in cholesterol on the ER and is thought to regulate lipid transport from the ER to the plasma membrane; treatment with (+)-pentazocine causes these sigma-1 receptor-containing microdomains to disappear (Hayashi and Su, 2003). In normal, agonist-free conditions, the sigma-1 receptor at the ER is bound to binding of immunoglobulin protein (BiP), a molecule involved in the response to unfolded proteins. It was observed in CHO cells that upon calcium depletion

(by ATP via P2Y receptors, by treatment with thapsigargin, or by treatment with the calcium chelator BAPTA), the S1R dissociates from BiP and forms complexes with IP$_3$R3. Treatment with (+)-pentazocine after thapsigargin-mediated calcium depletion increases the coupling between S1R and IP$_3$R3 (Hayashi and Su, 2007). A previous study suggested that ankyrin B (particularly the ankyrin 220 isoform), IP$_3$R3, and the S1R associate in the ER (see Figure 2.3). Treatment with (+)-pentazocine evoked dissociation of S1R from ankyrin B and presumably IP$_3$R3, since this treatment also caused the S1R to disappear from the P3L (ER-enriched) fraction and translocate to the plasma membrane (Hayashi and Su, 2001).
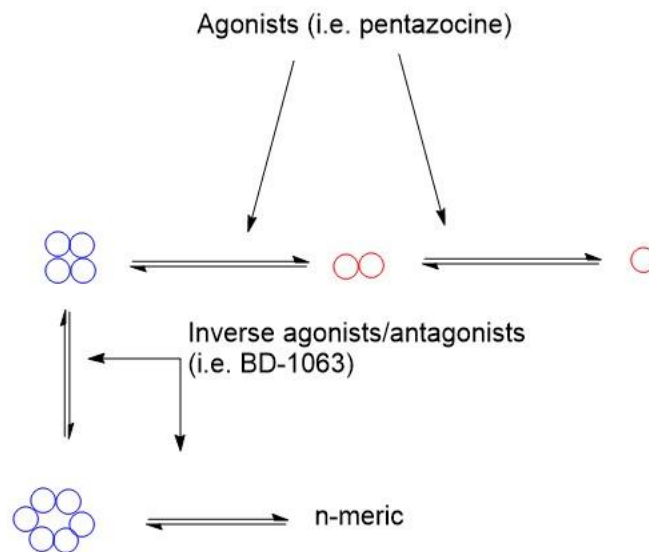
Figure 2.3 Agonists promote the formation of lower order oligomers which can interact with other protein clients. Inverse agonists and antagonists promote the formation of higher-order oligomers which represent the inactive state of the receptor (Chu and Ruoho, 2016). Red circles represent the states that can interact with protein clients while blue represents the inactive state.
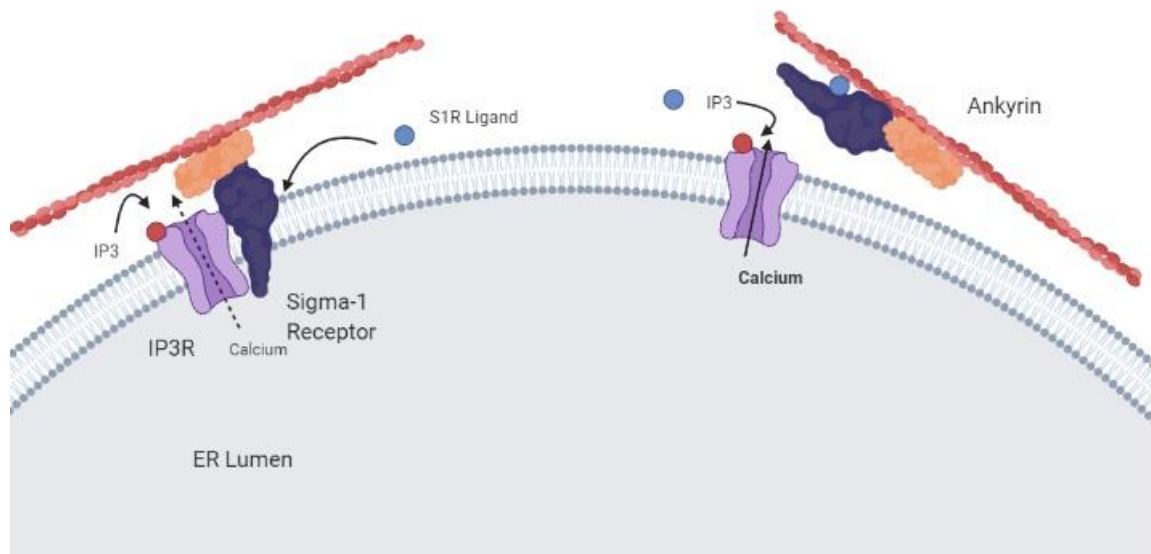
Figure 2.4 The interaction between IP$_3$R3, the sigma-1 receptor, and ankyrin occurs in the basal, unstimulated state. Upon sigma-1 receptor binding (blue circle), ankyrin and the sigma-1 receptor dissociate from IP$_3$R3 and this allosterically potentiates IP$_3$R3, increasing efflux of calcium. Since IP$_3$ (red circle) concentrations at basal state are not high enough to stimulate efflux of calcium, there would initially be no calcium release. Upon addition of the sigma-1 receptor agonist, the IP$_3$R becomes more sensitive to intracellular IP$_3$ concentration. This may enable the IP$_3$R receptor to become active in basal state, but evidence suggests that G$_q$-coupled receptor stimulation is required to fully observe the potentiating effect of the sigma-1 receptor (Hayashi and Su, 2001). Image created in Biorender.

Sigma-1 receptor ligands can also regulate the homo-oligomeric status of the S1R (Chu and Ruoho, 2016). In physiological conditions, the intracellular population of the S1R is distributed among monomeric and oligomeric states. There is evidence that the S1R may be constitutively active, based on findings that demonstrated that the sigma-1 receptor can release inhibition of G-protein mediated signaling; overexpression of the sigma-1 receptor can increase bradykinin-mediated intracellular calcium release in the absence of agonists for the bradykinin receptor. Inverse agonists like BD-1063 bias the population S1R towards higher order oligomers while agonists bias the population of lower order oligomers (Figure 2.3). The dimers are thought to allow S1R to form chaperone complexes, while the monomers are thought to allow S1R to form chaperone complexes and complexes with protein partners (Chu and Ruoho, 2016). It was also demonstrated that sigma-1 receptor agonists can induce translocation of the sigma-1 receptor to focal adhesion contacts at the

41

plasma membrane in CHO cells (Mavlyutov and Ruoho, 2007). Interestingly, stabilization of F-actin filaments dramatically enhanced the number of S1R at the plasma membrane, suggesting that the actin cytoskeleton may play a role in translocation of the S1R.

2.4.2 Sigma-1 Receptor and IP$_3$ Receptors

As stated in the previous section, the sigma-1 receptor responds to calcium depletion in the ER by increasing its coupling with IP$_3$R3. Moreover, sigma receptor agonists induce dissociation of the S1R and IP$_3$R from ankyrin B (Hayashi and Su, 2001). This dissociation alone was not found to increase cytosolic calcium concentrations, however, in the presence of an agonist for a G$_q$-coupled receptor (bradykinin) of thus, presumably increased IP$_3$ concentrations, various sigma-1 receptor agonists enhanced the increase in cytosolic calcium (although it has been observed that the sigma-1 receptor agonist BD-737 alone can increase IP$_3$ synthesis in cardiac myocytes; see Novakova et al., 1998). In the work by Hayashi and Su in 2001, it was determined that dissociation of ankyrin from IP$_3$R increased the binding of [^{3}H]IP$_3$, suggesting that sigma-1 receptor-mediated dissociation of ankyrin from IP$_3$R can potentiate calcium efflux from the ER by increasing binding of IP$_3$ to IP$_3$R. The potentiation of bradykinin-induced calcium release was determined to occur in a bell-shaped manner with respect to S1R agonist concentration, and was unaffected by removing calcium from the bath solution (Hayashi et al., 2000). Importantly, three different agonists (PRE-084, pentazocine, and pregnenolone sulfate) of the S1R increased bradykinin-potentiated calcium release from the ER. The effect of PRE-084 on intracellular calcium was abolished by the S1R antagonist NE-100 and the effects of the other ligands were abolished by knockdown of the S1R. In these experiments, no potentiating effect on intracellular IP$_3$ concentration was observed, although (+)-pentazocine increased the ceiling of bradykinin-induced IP$_3$ formation. Although discussion of the protein chaperone role of the sigma-1 receptor is beyond the scope of this manuscript, it should be noted that the sigma-1 receptor prevents proteasomal degradation of the IP$_3$ receptor. Knockdown of the sigma-1 receptor revealed prominent proteasomal degradation of IP$_3$R3 upon ATP stimulation of P2Y2 receptors

(Hayashi and Su, 2007). Thus, the sigma-1 receptor modulates IP$_3$R3 at multiple levels. It can directly enhance activation of IP$_3$R3 and it can also prevent degradation of IP$_3$R3.

2.4.3 Sigma-1 Receptor and Store-Operated Calcium Entry (SOCE)

When intracellular stores of calcium are depleted, STIM1 detects the drop in ER calcium concentration and translocates to the plasma membrane-ER junction where it binds to the calcium channel Orai1. To deplete HEK cells of intracellular calcium stores, the cells were treated with thapsigargin in calcium free media. Subsequently, calcium was added to the media and intracellular calcium concentration was measured. This technique effectively measures the degree of SOCE. It was found that in HEK cells transfected with S1R, the increase in intracellular calcium subsequent to addition of calcium to the media was blunted compared to cells not expressing S1R. A similar effect was observed in cells treated with carbachol and ATP (these compounds trigger endogenous depletion of ER calcium). To investigate whether ligands of S1R can modulate the S1R-mediated effects on SOCE, cells were treated with the S1R agonist SKF10047 and the S1R antagonist BD-1047. It was observed that the antagonist enhanced SOCE while the agonist inhibited SOCE in HEK and CHO cells transfected with S1R. Coimmunoprecipitation assays revealed that S1R associates with STIM1 and that treatment with a S1R agonist increases this association while treatment with a S1R antagonist decreases it. Upon calcium depletion, the STIM1-S1R complex translocates to the ER-plasma membrane interface, where it associates with Orai1. The sigma-1 receptor decreases the speed at which this translocation occurs and additionally inhibits association with Orai1. It was determined that the S1R exerts its effects via STIM1 rather than via association with Orai1 (Srivats et al., 2016).

2.4.4 Sigma-1 Receptor and the Actin Cytoskeleton

Following the finding that sigma-1 receptor activation mediates dissociation of IP$_3$R3 from ankyrin (Hayashi and Su, 2001), it was proposed that cocaine may mediate changes to the spectrin-actin cytoskeleton via the sigma-1 receptor (Su and Hayashi, 2000). Ankyrin is an adaptor protein that is normally bound to the spectrin component of the actin-

spectrin cytoskeleton. Specifically, spectrin serves as a crosslinker between actin filaments, forming the mesh that gives the plasma membrane definition. Ankyrin, as an adaptor protein, connects spectrin to other membrane proteins and cell adhesion molecules. This dissociation results in increased flux of calcium ions from the ER due to enhanced binding of IP_3 to IP_3R3. The dissociation mediated by cocaine as a ligand has been observed to be persistent for up to two hours, suggesting this dissociation may not be transient in nature. Calcium can modulate the interaction between spectrin and actin (Tanaka et al., 1991). Hayashi and Su also proposed that cocaine-mediated modulation of intracellular calcium due to activation of G_q-coupled $D1_x$ receptors may also modulate the cytoskeleton. It was specifically proposed that these changes in the cytoskeleton can affect the architecture of dendrites and dendritic spines, but it may be equally plausible that these same changes occur in astrocytes.

2.5 Distribution of the Sigma-1 Receptor in the Rat NAcc and PrL

2.5.1   Background

The sigma-1 receptor is expressed in many tissues including the brain, heart, lungs, and liver. It is well known that neurons express the sigma-1 receptor. Previous immunohistochemical data suggests that the S1R is moderately expressed by neurons and ependymocytes throughout the brain, including the striatum. However, in this report, there was no sigma-1 receptor staining within astrocytes (Alonso et al., 2000). In this report, sigma-1 immunoreactivity detected via electron microscope was punctate and located in the perikaryal and dendrites of neurons, with a distinct absence of any immunoreactivity in the axons. Nevertheless, more recent data has come to light suggesting that both neurons and astrocytes in the striatum express the sigma-1 receptor modestly (Francardo et al., 2014). If indeed the sigma-1 receptor is expressed in astrocytes, then it is plausible that sigma-1 receptor agonists can promote morphological alterations by its interactions with the actin cytoskeleton and IP_3R (Hayashi and Su, 2001). Indeed, *in vitro* and *in vivo* treatment with METH in mice increases astrocyte reactivity (indicated by stellation and

increased GFAP expression). Moreover, addition of METH to astrocyte-neuron cell cultures enhanced intracellular calcium release evoked by glutamate and dopamine (Narita et al., 2005). Whether these METH-mediated alterations are dopamine-mediated, S1R-mediated, or both is still an open question in the field.

In order for the S1R to be relevant to astrocytic physiology, it must be expressed by astrocytes. Given the conflicting literature regarding expression of S1R by astrocytes, the present experiment was designed to probe the expression of the S1R by astrocytes. The prelimbic cortex and the nucleus accumbens were selected due to their involvement in mediating drug-seeking behavior.

<h2 style="text-align:center">2.5.2 Materials and Methods</h2>

Male Sprague-Dawley rats weighing between 322 and 566 grams were deeply anesthetized using ketamine/xylazine/acepromazine and transcardially perfused first with cold 4% paraformaldehyde (PFA) and cold 1X phosphate-buffered saline (PBS). The brains were removed and 1 mm thick sections were cut on the vibratome (Leica VT1200) containing the PFC and nucleus accumbens in 1X PBS. The thick sections were cryoprotected for two days in 30% sucrose (prepared in 1X PBS). They were then frozen on the cryostat at -16°C and sliced into 50 µm thick sections. The 50 µm thick slices were placed into a freezer storage medium consisting of the following: 30% w/v sucrose in a solution containing 300 mL of ethylene glycol, 300 mL of glycerol, and 300 mL of 1X PBS.

The 50 µm sections were thawed at 4 degrees Celsius, placed in 15% sucrose (in 1X PBS) for 15 minutes, and then washed in 1X PBS three times for 10 minutes. Two different primary antibody cocktails were used, one containing 1:1000 rabbit anti-Sigma1 receptor (Abcam, ab53852) and 1:1000 goat anti-GFAP (Abcam, ab53554) while the other contained 1:1000 mouse anti-NeuN (Novus Biologicals, NBP1-92693) and 1:1000 rabbit anti-Sigma1 receptor. These two different groups are called Group GSD (GFAP, Sigma-1, and DAPI) and NS (NeuN and Sigma-1). Both were prepared in an antibody dilution buffer

containing 3% normal donkey serum in 1X PBS with 0.2% Triton X-100. First, the slices were blocked in a solution of 10% v/v normal donkey serum and 0.2% Triton X-100 in 1X PBS for 30 minutes. Subsequently, the primary antibody cocktail was added, and the slices were allowed to incubate overnight at 4 degrees Celsius. After overnight incubation, the slices were washed 3x10 minutes in 1X PBS and blocked again using a blocking buffer serum from the same animal as the host identity of the subsequent secondary antibody. For slices stained with anti-NeuN, normal goat serum was used while for slices stained with anti-GFAP, normal donkey serum was used. Donkey anti-goat A647 (Abcam, ab150135), goat anti-rabbit or goat anti-mouse A405 (Thermo-Fisher, A31553) were used. Slices were incubated with each secondary antibody for 2 hours at room temperature. After washing 3x10 minutes, the slices were blocked with normal goat serum-containing blocking buffer and incubated with goat anti-rabbit A594 (Abcam, ab150088) for 2 hours at room temperature. Slices stained with GFAP were incubated with 2.86 µM DAPI for 10 minutes and then washed 3x10 minutes with 1X PBS-T (0.2% Triton X-100 in 1X PBS). Slices strained with NeuN were washed 3x10 minutes with 1X PBS. All slices were then mounted and coverslipped using Prolong Gold Antifade or Prolong Diamond Antifade.

For image acquisition, the Nikon A1R confocal microscope was used. The pinhole diameter was set at 1.2 AU for all samples. The general region of interest (prelimbic cortex or nucleus accumbens) was identified using the 10x (air-immersion) and 20x (water-immersion) objectives. Initial gain and power settings for each channel are displayed in *Table 2.1*. At all times, the gain was 30x higher than the power of the laser. Images were taken with 4x line averaging at resolution 1024x1024. First a large tiled image was taken using the 40x objective, then the area of interest was identified and a z-stack with slices spaced 1 µm apart (ranging from 10-12 µm total per stack) was taken. The resulting ND2 files were saved and imported to NIS-Elements for processing. Background was subtracted using the rolling ball method and images were deconvolved for 10 iterations using the blind method of 3D deconvolution. After image acquisition, all slices were visualized using the 10x bright field objective on the AxioScan slide scanner. Slices that did not contain the nucleus accumbens or the prelimbic cortex were excluded from analysis.

Table 2.1 The initial gain and power settings utilized to visualize immunostained tissue

	HV (gain)	**Power**
647 nm	90	3
561 nm	90	3
405 nm	150	5

Data analysis was conducted using Fiji ImageJ. First, either DAPI-positive or NeuN-positive cells were counted using the multi-point tool. For tissue stained with anti-GFAP, subsequently, all astrocytes with visible nuclei were counted. The criterion for inclusion as an astrocyte were: GFAP immunoreactivity must fully or partially surround the DAPI staining and the identified cells must have two or more visible processes projecting from them. The criteria for identification as a neuron was simply round NeuN immunoreactivity. For a cell to be considered positive for the sigma-1 receptor, 3 or more puncta had to be present within the GFAP/DAPI+ or NeuN+ area. Statistical analysis (two sample t-tests assuming unequal variance) was conducted in GraphPad Prism. Total cell count was calculated by counting all cells in a z-stack and dividing by the volume enclosed by the z-stack. Proportions were calculated by dividing one category in the total cell count by another.
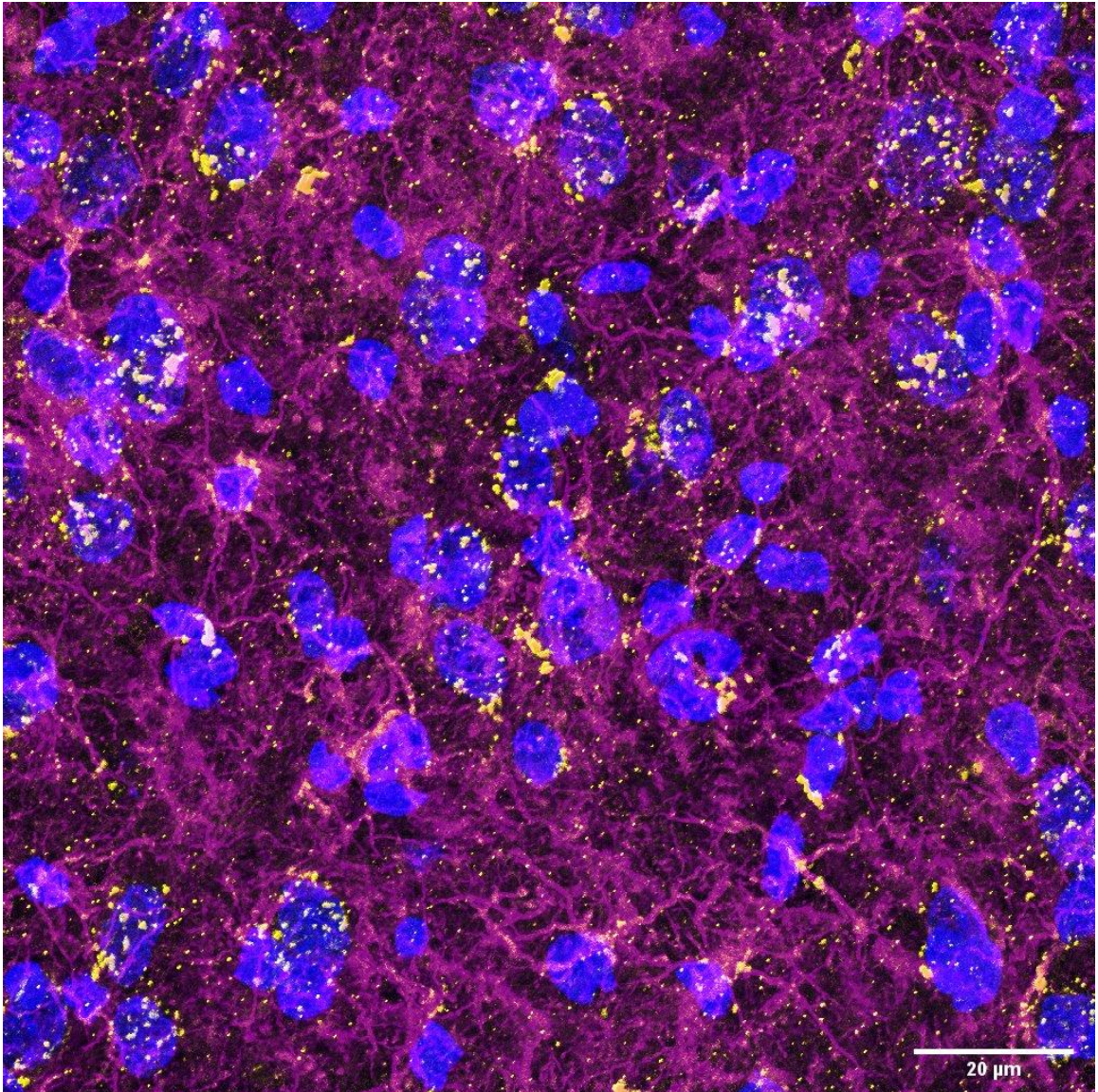
Figure 2.5 A maximum intensity projection of a NAcc slice; GFAP (magenta), Sigma1 receptor (yellow), and DAPI (blue). Z-stack thickness: 11 µm.
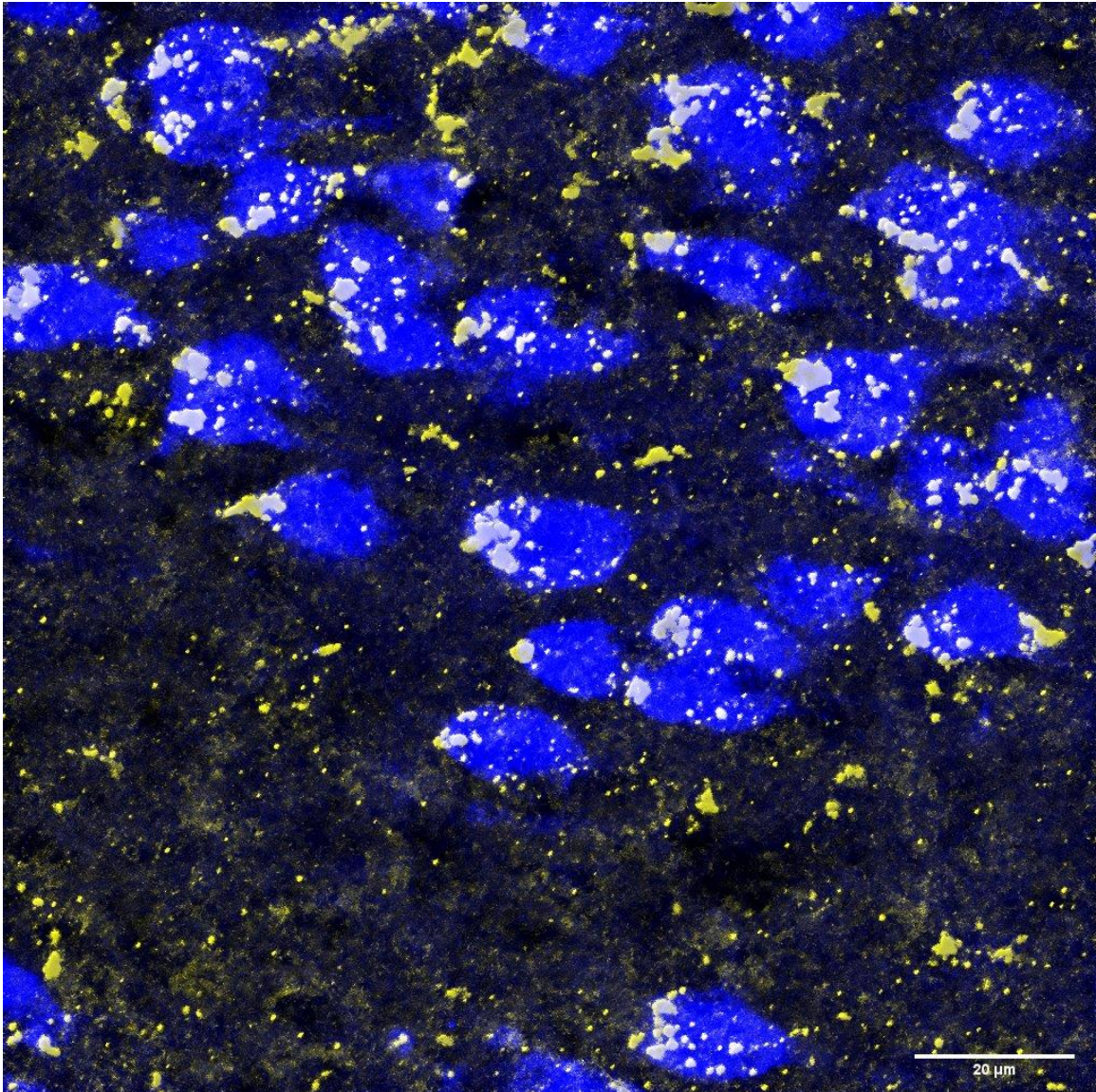
Figure 2.6 A maximum intensity projection of a NAcc slice; NeuN (blue) and Sigma1 (yellow)

For total cell count analysis of NAcc slices in group NS there were n = 10 slices and n = 7 in group GSD included in the analysis. For analysis of PrL slices, in group NS, there were n = 6 slices and in group GSD, there were n = 6 slices. These slices came from two animals. The total cell count revealed a significantly greater density of DAPI-positive cells in the nucleus accumbens versus the prelimbic cortex (p < 0.05) and a significantly greater density of DAPI-stained cells with sigma-1 receptor immunoreactivity (group

GSD; $p < 0.05$) in the nucleus accumbens versus the prelimbic cortex. All total count data is presented in Figure 2.7. Astrocytes in both the nucleus accumbens and prelimbic cortex possessed characteristic sigma-1 receptor immunoreactivity in their processes (Figure 2.9). In NS slices, sigma-1 receptor immunoreactivity was distributed throughout the cytosol and on the plasma membrane of neuronal cell bodies (Figure 2.10). No significant differences between regions were found when analyzing the proportion of cells that were sigma-1 receptor immunoreactive (Figure 2.8). In both the PrL and the NAcc, approximately 73% of DAPI stained nuclei contained clustered puncta of sigma-1 receptor immunoreactivity. Interestingly, on average, almost all (97.8%) neurons in both regions expressed the sigma-1 receptor, while most, but not all (91.2%) GFAP-positive astrocytes expressed the sigma-1 receptor.
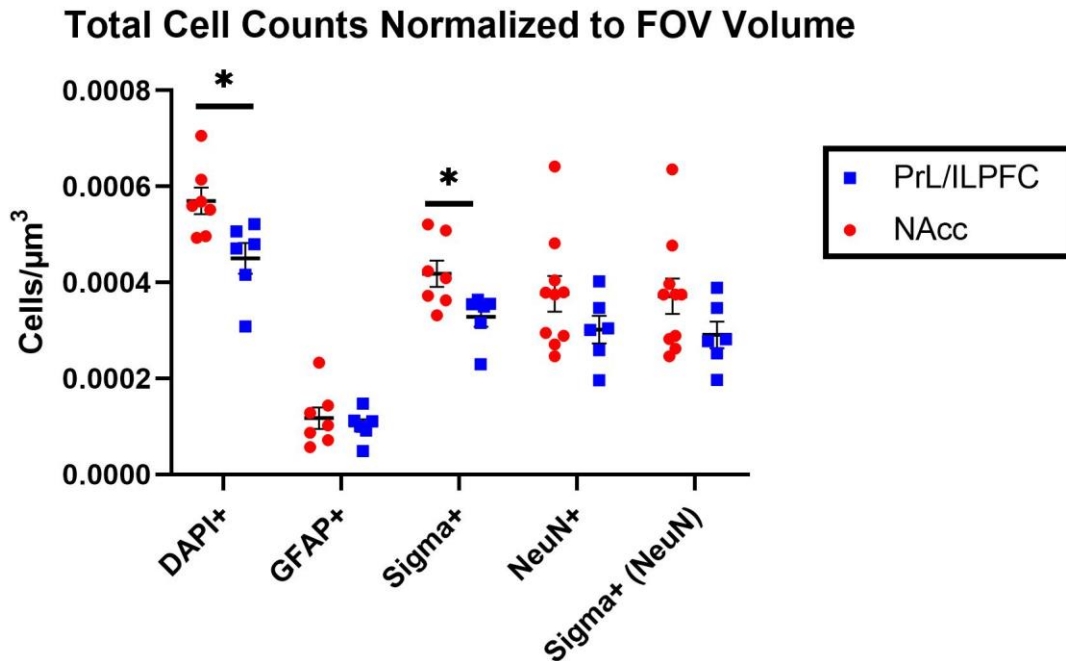
Figure 2.7 A graph showing the total cell counts. Note that the Sigma+ category denotes sigma-1 receptor-positive cells in GSD slices while Sigma+ (NeuN) denotes cells in NS slices

50

Proportion of Sigma-1 Expression
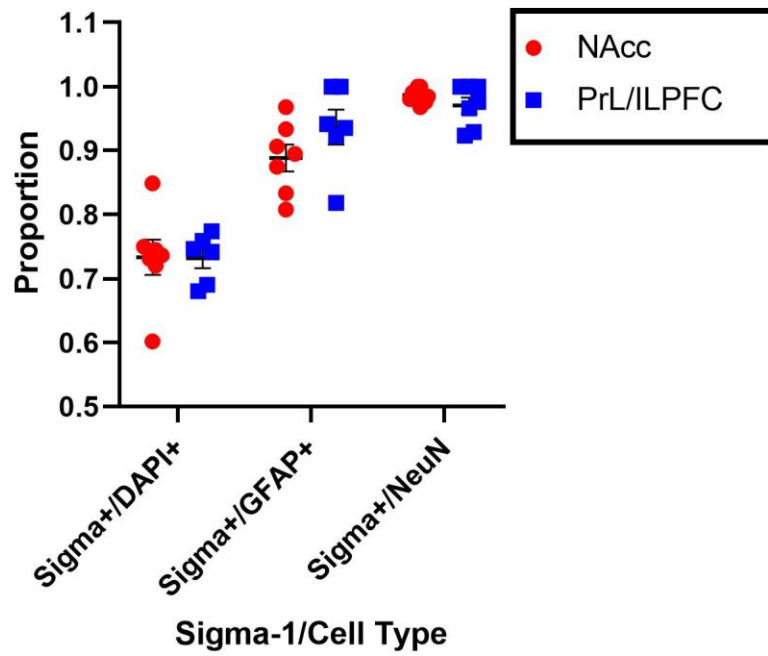
Figure 2.8 A graph showing proportions. Here, the proportion represents the number of cells positive for type A (i.e. sigma-1 receptor immunoreactivity) out of cells positive for type B (i.e. DAPI+ cells). No statistically significant differences were noted between regions.
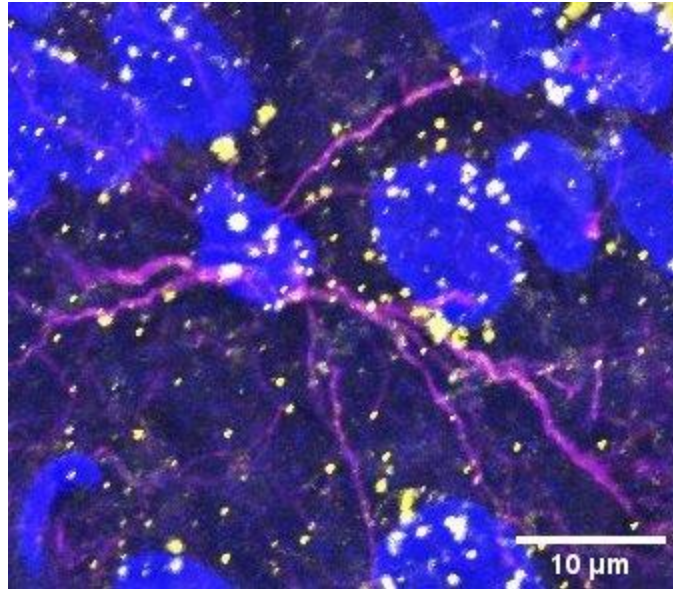
Figure 2.9 A maximum-intensity projection image of a single astrocyte in the nucleus accumbens taken with the 60x oil-immersion objective. Note both perinuclear (blue indicates DAPI) and peripheral sigma-1 receptor immunoreactivity (yellow) in the astrocyte (magenta) or on the membrane of its processes.
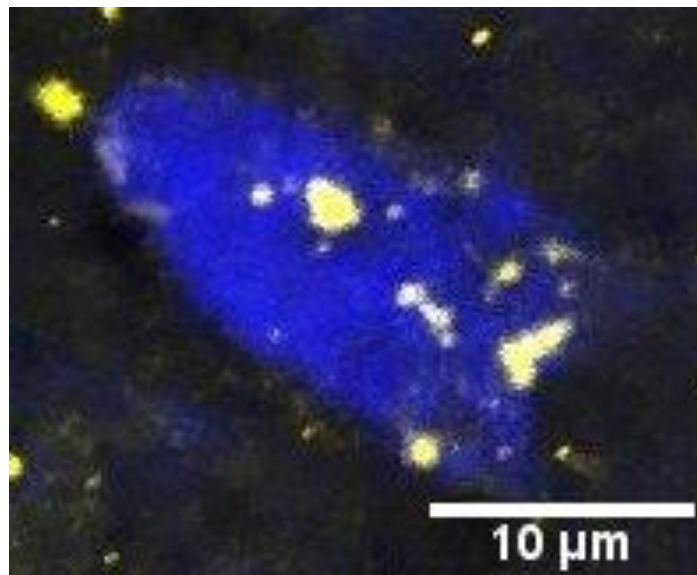
Figure 2.10 A maximum-intensity projection image of a neuron (blue is NeuN immunoreactivity) in the nucleus accumbens with sigma-1 receptor immunoreactivity (yellow) inside the cytosol/nucleus and along the surface of the cell body. Image taken with the 40x water-immersion objective.

2.5.4 Discussion

In conclusion, we note that like Francardo and coworkers, there is detectable and significant sigma-1 receptor density in astrocytes of the striatum, particularly in the nucleus accumbens. It is possible that the antibody prepared by Alonso and coworkers (Alonso et al., 2000) does not bind the sigma-1 receptor with high enough avidity (the total binding strength at every binding site on the antibody) or affinity to detect the levels of expression within striatal astrocytes. Indeed, they reported low to medium-intensity sigma-1 receptor immunoreactivity in the striatum, in stark contrasts with results that we and others have found (Francardo et al., 2014). It may also be possible that the use of a confocal microscope by ourselves and Francardo et al. permitted greater resolution than the images obtained by Alonso and coworkers. The source of this discrepancy remains unknown. Nevertheless, here, we demonstrate conclusively that astrocytes in the nucleus accumbens and the prelimbic cortex express the sigma-1 receptor.

The increased DAPI+ cell count in the nucleus accumbens versus the prelimbic cortex suggests a greater cell density in the nucleus accumbens. The greater number of sigma-1 receptor immunoreactive cells in the nucleus accumbens and prelimbic cortex versus the number of astrocytes counted suggests that many other cells (including astrocytes that do not express GFAP) also express the sigma-1 receptor. The increased total cell count of sigma-1 receptor immunoreactive DAPI-positive cells is not reflected in the analysis of the proportion of sigma-1 positive cells, suggesting that the increased total sigma-1 immunoreactive DAPI-positive cell count may simply be a product of increased cell density in the nucleus accumbens. However, it should be noted that GFAP expression is highly heterogeneous and that striatal astrocytes typically express less GFAP mRNA relative to hippocampal astrocytes (Chai et al., 2017). Thus, it is plausible that a subset of the DAPI-positive, S1R-positive cells are really astrocytes that do not express GFAP.

There are several limitations to this experiment. First is the fact that the number of channels on the Nikon A1R in confocal mode limits the number of different antibodies that can be used on a single slice. Ideally, both NeuN and GFAP would be labelled in the slices in addition to the Sigma-1 receptor, and the nuclei of NeuN and GFAP-positive cells would also be visible. However, this could not be accomplished due to the limited number of channels on the confocal microscope. While it is theoretically plausible to use the goat anti-mouse A405 antibody in conjunction with the donkey anti-goat A647 and goat anti-rabbit A594 antibody, this would have meant that DAPI could not be used. Detection of cell nuclei is important for counting astrocytes, as their convoluted morphology makes it difficult to distinguish one astrocyte from the other. Second, the small sample size limits statistical analysis because it is not possible to account for potential animal to animal differences: only two rats were sacrificed to generate these slices. In order to determine the influence of animal-to-animal variability on these results, a larger number of animals and a larger number of sections should have been used.

CHAPTER 3. SIGMA-1 RECEPTOR-MEDIATED EFFECTS OF
METHAMPHETAMINE IN ACUTE STRIATAL SLICE PREPARATIONS FROM THE
RAT

3.1 Background

From the previous experiment, we have concluded that there is robust expression of the sigma-1 receptor in both astrocytes and neurons of the nucleus accumbens. The sigma-1 receptor is involved in mediating dopamine release in the mouse nucleus accumbens slice preparations. An indirect link between reactive oxygen species (ROS) via the sigma-1 receptor is suggested to contribute to dopamine release because both METH+BD-1063 and the antioxidant TEMPOL+METH reduced dopamine efflux relative to METH alone. It was found that VMAT2 was S-glutathionylated and that this S-glutathionylation can be blocked by incubation with the sigma-1 receptor antagonist BD-1063 (Hedges et al., 2018). Glutathionylation impairs VMAT2 function and thus enhances accumulation of dopamine in the cytosol. Although there is evidence of VMAT2 expression in astrocytes (Petrelli et al., 2018), generation of reactive oxygen species (ROS) and increased intracellular calcium release via the sigma-1 receptor activation by METH could have different effects on astrocytes than on neurons. It has already been described in the literature that extracellular dopamine modulates astrocyte morphology in a concentration-dependent manner (Galloway et al., 2018). Therefore, it is plausible that elevated dopamine release via the sigma-1 receptor can induce morphological alterations in astrocytes.

Since the sigma-1 receptor modulates the actin-spectrin cytoskeleton (Su and Hayashi, 2001) and intracellular calcium release enhanced by the actions of sigma-1 receptor could potentially affect the interaction between spectrin and actin (Tanaka et al., 1991), it is also plausible that direct activation of the sigma-1 receptor can modulate the morphology of astrocytes by directly altering the actin-spectrin cytoskeleton.

In the present experiment, we sought to determine the contribution of the sigma-1 receptor to changes in sigma-1 receptor distribution and astrocytic morphology. Although

we could not probe the effects of dopamine receptor activation, we were able to do so indirectly, as treatment with BD-1063 (Hedges et al., 2018) and PRE-084 (Sambo et al., 2017) have been shown to reduce dopamine release in slice preparation and dopamine neuron cell culture, respectively.

3.2 Materials and Methods

Two adult male Sprague-Dawley rats were deeply anesthetized with isoflurane and then decapitated. The brain was sectioned into 300 µm thick slices containing the striatum, particularly the nucleus accumbens as well as the caudate-putamen. Slices were incubated in aCSF (in mM: 2 $CaCl_2$, 3 KCl, 1 $MgCl_2$, NaH_2PO_4 1.25, $NaHCO_3$ 26, and d-glucose 10) until all necessary slices were cut. The slices were transferred to solutions according to Table 3.1; all solutions were prepared in aCSF. The concentration of PRE-084 used was derived from Sambo et al., 2017. The concentration for BD-1063 was taken to be a saturating concentration from Zhang et al., 2017. The concentration of METH used was calculated from results indicating the physiological mass of methamphetamine per unit mass of brain tissue derived from experiments in which rats were given 1 mg/kg of methamphetamine (i.v., Riviére et al., 2000). The slices were incubated for 2 hours at 37 °C before they were removed and placed in 4% paraformaldehyde in 1X PBS. After 3 hours of fixation, the slices were transferred to 30% sucrose in 1X PBS for cryoprotection and allowed to cryoprotect until the slices sank in the medium.

Table 3.1 All solutions used to incubate the slices from two different animals

	Meth (24.7 µM)	aCSF
BD-1063 (49.5 µM)	300 µm (n = 3 slices)	Not collected
PRE-084 (9.9 µM)	300 µm (n = 1 slice)	300 µm (n = 1 slices)
aCSF	300 µm (n = 1 slice)	300 µm (n = 1 slices)

From the 300 µm slices, 50 µm thick sections were cut on a cryostat (Leica CM 1860) and placed into freezer storage medium. When IHC was conducted, the sections were thawed at 4 ℃ and then transferred to 15% sucrose solution. The slices were then transferred to 1X PBS and washed 3x10 minutes. They were then blocked in blocking buffer (10% NDS and 0.2% Triton X-100 in 1X PBS) and then incubated with primary antibody cocktail [1:1000 polyclonal rabbit anti-Sigma1 (Abcam, ab53852) and 1:1000 polyclonal goat anti-GFAP (Abcam, ab53554) in 3% NDS, 0.2% TX-100, and 1X-PBS] overnight at 4 ℃.

After incubation with the primary antibodies, the slices were washed 3x10 minutes with 1X PBS at room temperature. They were then blocked in blocking buffer made from NGS rather than NDS for 30 minutes. After protecting the slices from light and removing the blocking buffer, 1:400 polyclonal goat anti-rabbit A594 (buffer composition: 3% NGS and 0.2% Triton X-100 in 1X PBS; Abcam, ab150088) was added and the slices were incubated for 2 hours at room temperature. Subsequently, the slices were washed 3x10 minutes with 1X PBS and blocked again with blocking buffer made from NDS. The slices were incubated with 1:400 polyclonal donkey anti-goat A647 (Abcam, ab150135) for 2 hours. They were then washed 3x10 minutes with 1X PBS and transferred to DAPI working solution (2.86 µM DAPI in PBS-T consisting of 0.2% TX-100 in 1X PBS). Following incubation for 10 minutes, the slices were washed 3x10 minutes in PBS-T. They were then mounted and coverslipped with Prolong Diamond Antifade.

All images were acquired on the Nikon A1R confocal microscope with a pinhole diameter of 1.2 AU and image resolution of 1024x1024 using a 60x oil-immersion objective (NA: 1.4) with 4x line averaging. The power of the laser and the gain was set such that gain was always 30x greater than the power (initial settings were identical to those displayed in table 2.1). Since some slices contained the nucleus accumbens and others did not, the images are of areas within the caudate putamen. Large, stitched images of all the slices can be seen in Figure 3.1 while maximum intensity projection images can be seen in Figure 3.2.
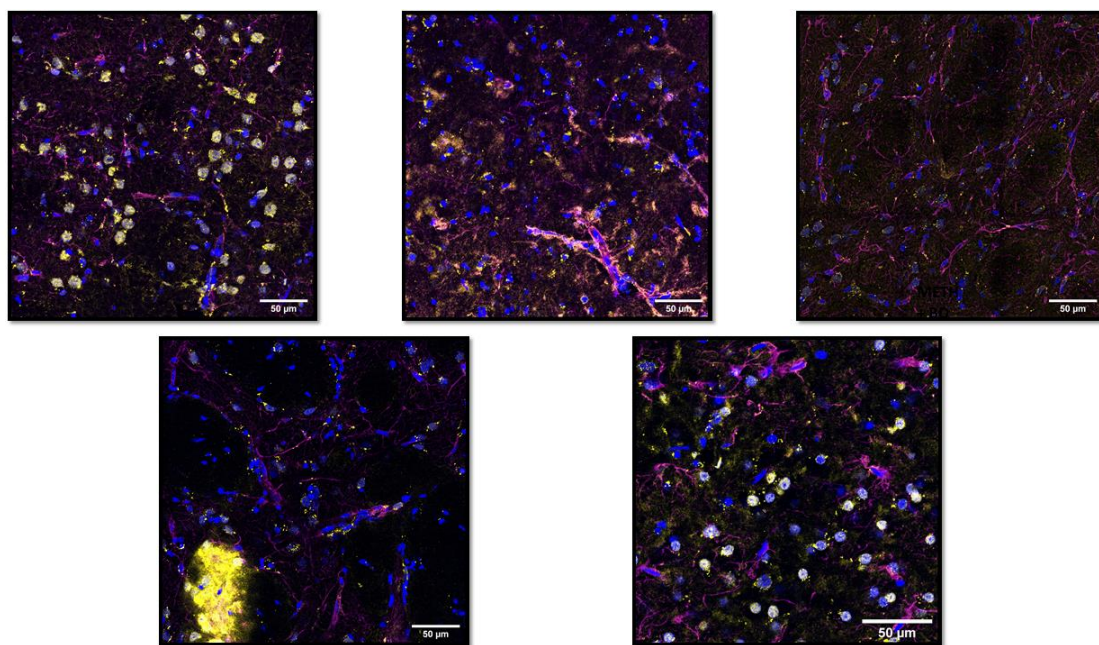
Figure 3.1 Large stitched images of striatal tissue; DAPI (blue), anti-Sigma1 receptor (yellow), and anti-GFAP (purple). Top left: aCSF; top middle: METH; top right: METH + BD-1063; bottom left: METH + PRE; bottom right: PRE
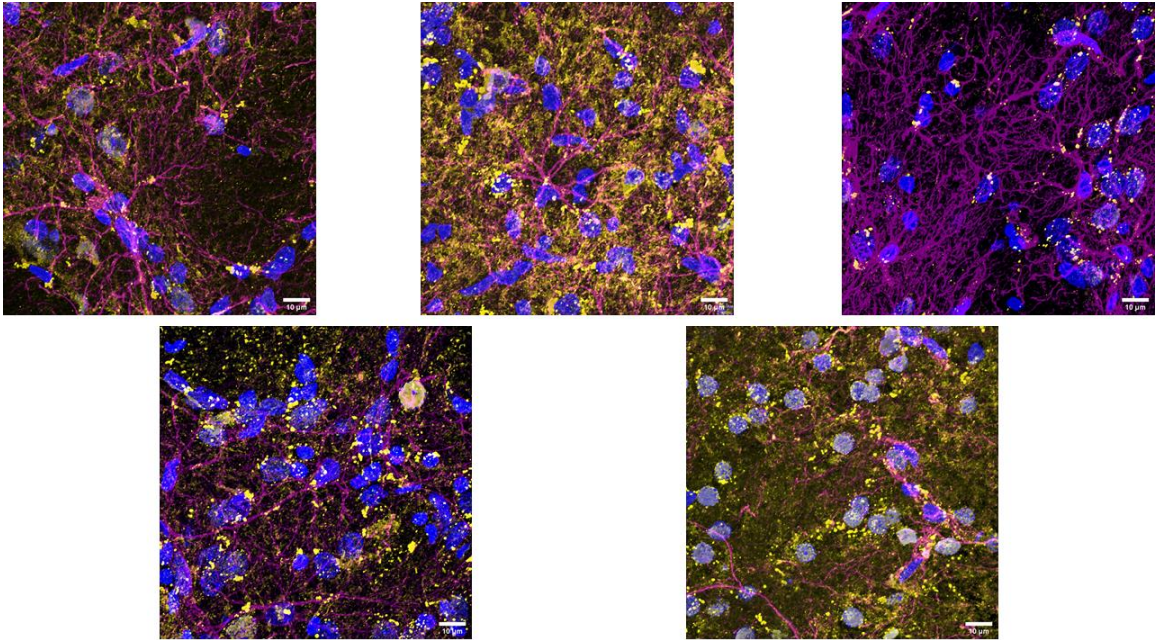
Figure 3.2 Representative images showing the maximum intensity projection of each slice (z-projection was taken of 6 slices or 6 µm containing the most astrocytes, hence the differences in background); DAPI (blue), anti-Sigma1 receptor (yellow), and anti-GFAP (purple). Top left: aCSF; top middle: METH; top right: METH + BD-1063; bottom left: METH + PRE; bottom right: PRE

For analysis of sigma-1 receptor puncta, first all DAPI and GFAP+ cells were counted in each slice using Fiji ImageJ. Analysis was conducted on slices such that the sample size was at least 15 astrocytes per group. The number of sigma-1 receptor puncta within each cell was counted. Any puncta on or adjacent to the DAPI-stained nucleus was categorized perinuclear while puncta in the processes were categorized as peripheral. An example of the puncta counting Only puncta within the DAPI+ or GFAP+ area were counted. For reconstruction of astrocytes, Bitplane Imaris 9.6 was used to generate a surface for 5 cells per slice. For all cells, only the largest continuous surface encircling the nucleus was considered to limit inclusion of processes from other astrocytes. Processes were counted using the 3D reconstruction of each cell and only processes extending from the cell body of an astrocyte were counted.

The (+)-methamphetamine hydrochloride was purchased from Cayman Chemical (#13997), PRE-084 from Sigma-Aldrich (P2607), and BD-1063 from Tocris (#0883). The composition of the cutting solution was, in mM: 2 $CaCl_2$, 3 KCl, 1 $MgCl_2$, NaH_2PO_4 1.25, $NaHCO_3$ 26, d-glucose 10, sucrose 219. All reagents were used without further purification.

All statistics were calculated in GraphPad Prism 8.4.3. To assess homogeneity of variance, Bartlett's test and the Brown-Forsythe test were used. Based on the results from the tests for differences in variance, homogeneity of variance could be assumed for all analyses. Normal one-way ANOVA for the stellation count and the surface area to volume ratio where therefore used and normal two-way ANOVA was used for the puncta localization count. The method of Tukey was used to calculate adjusted p-values for multiple comparisons for all data. Error bars in all the graphs show SEM.

3.3 Results

The volume and cell surface area data were imported from Imaris. The ratio of surface area to volume has previously been used as a metric for astrocyte complexity in astrocytes virally transfected with AAV5 GfaABC1D-Lck-GFP (Testen et al., 2018). Since the fine astrocytic processes contribute to greater surface area than volume, increased surface area:volume ratio indicates an increase in these fine processes which in turn indicates astrocytic complexity. Here, the surface area:volume ratio is used similarly, but on anti-GFAP stained brain slices. One-way ANOVA revealed no significant difference was found between treatment groups on the surface area:volume ratio [$F_{4, 29} = 0.9317$; $p > 0.05$], suggesting that this metric may not be effective for analysis of GFAP-stained images (Figure 3.3. It is also plausible that the length of time for incubation of slices with drugs may have not been sufficient to evoke dramatic remodeling of the astrocytic cytoskeleton.
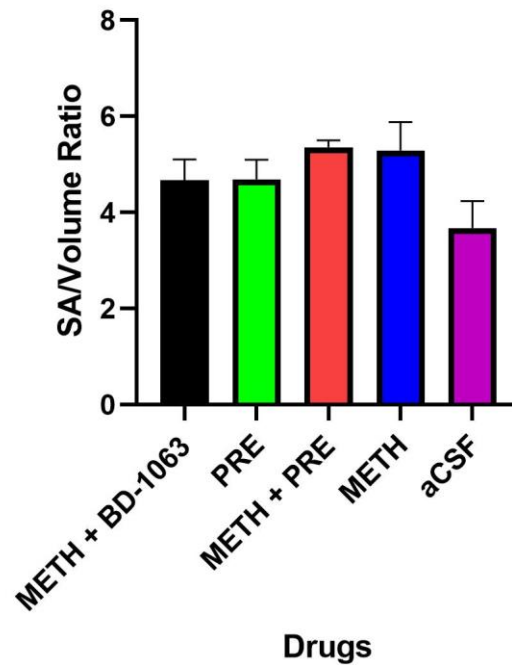
Figure 3.3 The surface area:volume ratio. Astrocytes were reconstructed on Imaris and the surface area and volume parameters were measured. There was no significant difference between groups (n=14 cells for BD+METH; n=5 cells for all other groups)

Astrocyte stellation was analyzed as the number of primary processes (stellations) were counted in Imaris by locating the nucleus and counting the number of GFAP+ processes extending radially from the nucleus (Figure 3.4) since the nucleus is contained by the cell body of astrocytes. Note that astrocytes *in vivo* are typically already stellate while astrocytes grown in culture are not usually stellate unless certain drugs are added to the media. One-way ANOVA revealed a significant difference between groups [$p < 0.05$; $F_{(4, 29)} = 3.913$]. The method of Tukey revealed a significant difference between the METH and the aCSF group ($p < 0.05$), with the METH astrocytes possessing a greater stellation count. Treatment of METH slices with the S1R antagonist, BD-1063, abolished the increase in stellation count ($p < 0.05$). However, treatment with the S1R agonist, PRE-084, alone did not alter the ramification count relative to the aCSF control. The combination of METH and PRE-084 reduced the ramification count relative to METH alone, but this result did not reach statistical significance.
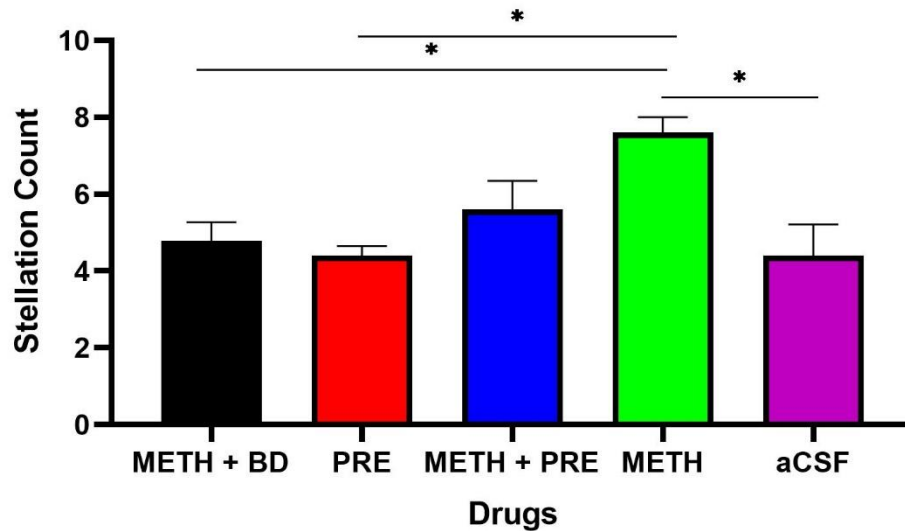
Figure 3.4 The stellation counts on reconstructed astrocytes. In addition to the significant difference between METH and aCSF, there was a significant difference ($p < 0.05$) between METH and METH + BD-1063 as well as a significant difference between PRE and METH ($p < 0.05$) revealed by multiple comparisons analysis.

Next, to assess whether the drug treatments altered the intracellular distribution of the sigma-1 receptor, sigma-1 receptor immunostained puncta were counted (Figure 3.5). Specifically, puncta within the nucleus or adjacent to the nucleus were counted as perinuclear while puncta in GFAP+ territory were counted as peripheral. Note that this type of analysis is not quantitative and that very bright clusters of puncta were counted as a single punctum. In all treatment groups, most astrocytes possessed both peripheral and perinuclear puncta, suggesting that in astrocytes, the sigma-1 receptor may be more widely distributed throughout the cell in basal state compared to neurons. A two-way ANOVA revealed significant main effects of treatment and localization [Treatment: $F_{(4, 214)} = 7.008$, $p < 0.0001$; Localization: $F_{(1, 214)} = 59.70$, $p < 0.0001$] as well as a significant interaction effect [$F_{(4, 214)} = 6.148$, $p < 0.005$]. Using the method of Tukey for multiple comparisons revealed no significant difference between groups for perinuclear puncta. However, there was a statistically significant ($p < 0.05$) increase in peripheral puncta for METH-treated slices versus aCSF-treated slices. This increase was abolished by addition of BD-1063 ($p < 0.0001$) and PRE-084 ($p < 0.001$). Contrary to observations in striatal neurons (Francardo et al., 2014), PRE-084 did not induce redistribution of the sigma-1

receptor relative to aCSF. In fact, in all samples, there were several puncta located in the processes of astrocytes, far from the nucleus. Curiously, when compared to the slice incubated with METH and PRE-084, the slice incubated in PRE-084 alone demonstrated markedly increased peripheral puncta ($p < 0.005$). Thus, both BD-1063 and PRE-084 abolished the effect of METH on intracellular distribution of the sigma-1 receptor.
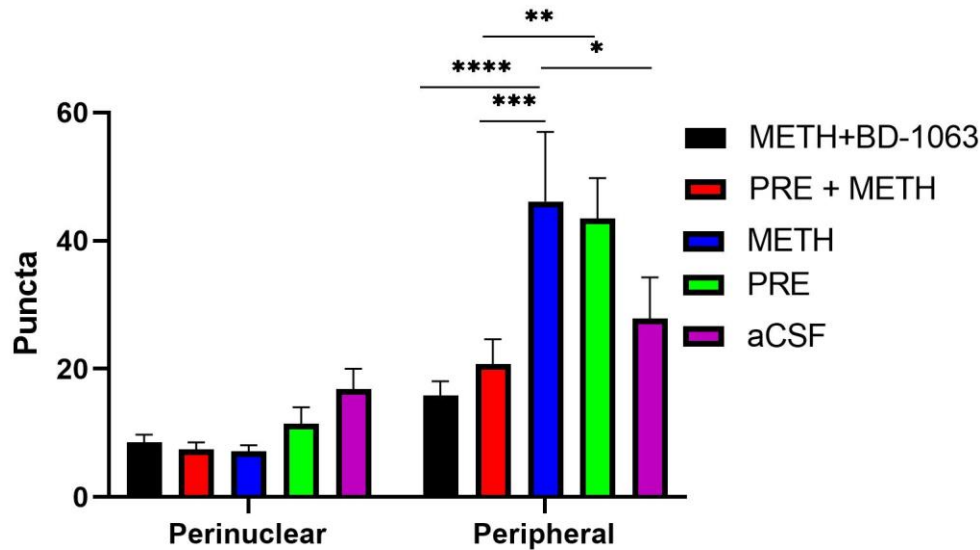
Figure 3.5 The puncta count data. No significant difference was found among treatment groups for perinuclear localization of the sigma-1 receptor.

3.4 Discussion

Methamphetamine administration has been shown to increase GFAP and sigma-1 receptor immunoreactivity (Zhang et al., 2015) in a manner that can be blocked by treatment with the sigma-1 receptor antagonist BD-1047. Here, we provide preliminary evidence that blockade of the sigma-1 receptor can also attenuate methamphetamine-induced increase in the stellation of astrocytes as well as the redistribution of sigma-1 receptors to the processes. Given that treatment of slices with PRE-084 alone did not induce an increase in stellation, it is likely that sigma-1 receptor activation is not sufficient to induce stellation. It is plausible that dopamine at dopamine receptors rather than methamphetamine at sigma-1 receptors initiates the morphological alterations. A study in astrocyte cell culture found that dopamine can induce rapid morphological and transcriptomic alterations via PARP1 activation of CTCF in a manner that can be blocked by D1 and D2 receptor antagonists (Galloway et al., 2018). However, in the case of methamphetamine, the present data suggests that the sigma-1 receptor is involved

somewhere in the pathway from dopamine receptor activation to morphological changes. The sigma-1 receptor may modulate signaling via dopamine receptors at several points along the signal transduction cascade. Since activation of the sigma-1 receptor can increase the affinity of IP_3 for IP_3R3, it is possible that binding of methamphetamine to the sigma-1 receptor and increased binding of dopamine to the phospholipase C-stimulating D1x receptor can potentiate calcium release from the ER and sigma-1 receptor activation can induce dissociation of IP_3R3 from ankyrin and the sigma-1 receptor which could alter the cellular cytoskeleton (Su and Hayashi, 2001). These experiments do not allow for the preclusion of direct sigma-1 receptor interaction with the D1x receptor. It has been demonstrated that the sigma-1 receptor can potentiate cAMP accumulation mediated by the canonical G_s-coupled D_1 receptor (Navarro et al., 2010). Thus, since the sigma-1 receptor forms oligomeric complexes with D1 receptors and also potentiates G_s-mediated signaling at the D1 receptor (Fu et al., 2010), it is also plausible that the sigma-1 receptor may act similarly with phospholipase C-stimulating dopamine receptors (D1x). See Figure 3.6 for a summary of hypothesized mechanisms by which methamphetamine can induce alterations in astrocytic physiology.

The surprising observation that PRE-084 attenuated redistribution of the sigma-1 receptor in slices also treated with METH may be a product of two phenomena: that PRE-084 attenuates METH-mediated dopamine release from neurons (Sambo et al., 2017) and that dopamine mediates increased stellation and therefore increased cross-sectional area. Since the technique employed in the present experiment utilized a manual count of the individual puncta regardless of intensity or size, it is plausible that an increased density of puncta in the METH+PRE condition made it difficult to discretize individual puncta. Instead of forming discrete puncta, a "lawn" of sigma-1 receptor immunoreactivity was observed. A simpler explanation is that PRE-084 is more potent at promoting the lower-order oligomeric states of the S1R, resulting in finer, more distributed puncta. This speculation is corroborated by findings suggesting that PRE-084 alone induces the formation of lower-order oligomers (Schmidt et al., 2018); This would mean, presumably, that finer puncta would be detected more easily than dense, bright puncta that may overlap and form intense clusters rather than discrete puncta. The converse may be true of the

M+BD condition; if BD-1063 induces the formation of higher order oligomers, clusters of sigma-1 receptor would appear to form fewer but brighter puncta.

There were several limitations to the present work. First, utilizing the same dilution of anti-GFAP antibody as was used in the previous experiment was not suitable for this experiment, in which excessive GFAP-positive staining impaired identification of individual astrocytes for 3D reconstruction. The small sample size limits the statistical power of the stellation count, since only five astrocytes per slice could be identified for morphological analysis in Imaris due to time limitations; future experiments should employ either thicker striatal slices for IHC or a larger cohort of animals. Moreover, it is unclear why the METH + PRE slice exhibited the marked decrease in peripheral sigma-1 receptor puncta. Lastly, in order to maximize the use of the slices, the entire striatum, the dorsal striatum was selected for analysis. It is possible that there may be regional differences in sigma-1 receptor expression. Indeed, differences have been observed in immunocytochemical studies assessing regional expression of the sigma-1 receptor. For example, Alonso and coworkers reported mild sigma-1 receptor immunoreactivity in the caudate/putamen but moderate sigma-1 receptor immunoreactivity in the nucleus accumbens (Alonso et al., 2000). Here, the striatum was treated as a whole and locations throughout the striatum were selected.
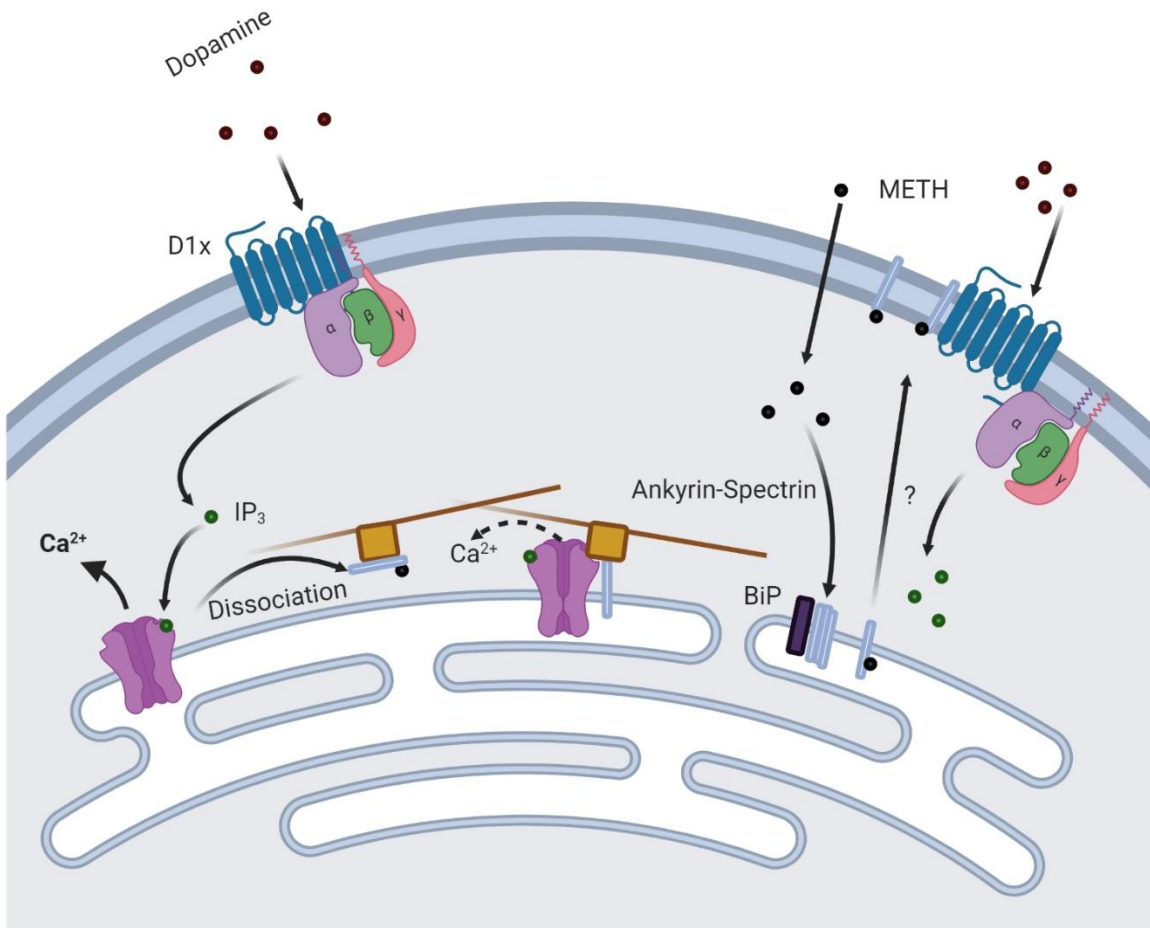
Figure 3.6 In the absence of sigma-1 receptor ligand, the sigma-1 receptor forms a complex between ankyrin, IP$_3$R3, and the spectrin/actin cytoskeleton. In the presence of METH (black circles), the IP$_3$R3 dissociates from ankyrin-spectrin which in turn potentiates IP$_3$ (green circles) binding to IP$_3$R3. This would shift the dose-response curve between calcium efflux and [IP$_3$] to the left, resulting in enhanced calcium efflux from the ER, particularly in the presence of phospholipase C signaling mediated by the D1x receptor. Binding of agonists to the sigma-1 receptor promotes lower order oligomeric states and dissociation from BiP. These lower order oligomeric states can translocate to the plasma membrane and interact with D1. Whether the resulting complexes exhibit enhanced coupling between receptor and G-proteins remains an open question

3.5 Future Directions

While these data provide preliminary evidence for the role of the sigma-1 receptor in methamphetamine-mediated alterations to astrocyte physiology in the dorsal striatum, it is unclear whether these alterations also occur in the ventral striatum. One report suggests that there is no change to the GFAP-positive processes immediately following self-administration of methamphetamine in the nucleus accumbens (Siemsen et al., 2019), however there are noted differences in astrocyte morphology after self-administered and experimenter administered methamphetamine (Narita et al., 2005). Thus, in order to clarify whether the changes to astrocyte morphology and sigma-1 receptor distribution occur in the ventral striatum, these experiments should be repeated in slices containing the nucleus accumbens. Moreover, given the morphological differences in astrocytes noted between methamphetamine self-administration and experimenter-administered methamphetamine, both methods of methamphetamine administration should be compared for effects on redistribution of the sigma-1 receptor.

Given that GFAP is not expressed in the fine astrocytic processes that constitute the majority of the surface area of astrocytes, utilization of both GFAP immunohistochemistry and virally-transfected astrocyte-specific fluorescent proteins may reveal details that could not be uncovered using the present method. For example, it is unknown whether the sigma-1 receptor can be found in the fine, GFAP-negative processes of astrocytes. If they can, then the puncta count data may represent an underestimate. Given that a manual count of sigma-1 receptor puncta in anti-Sigma1 immunostained tissue is not representative of the total expression of the sigma-1 receptor or the oligomeric status of the sigma-1 receptor (due to the nature of antibody binding to proteins and the diffraction limit of light microscopy), molecular approaches such as BRET would be more suited to investigate the precise oligomeric status of sigma-1 receptors and more quantitative approaches such as RT-qPCR could be used in future work to address the limitations of optical methods such as immunohistochemistry in the context of determining total sigma-1 receptor expression.

It is also noted that the present experiments cannot distinguish efficiently between dopamine-mediated changes to astrocytic morphology and sigma-1 receptor-mediated

changes to astrocytic morphology. Although PRE blocked METH-induced increases in stellation, it is not clear whether this decreased stellation occurs due to decreased dopamine release from neurons (Sambo et al., 2017) or direct action on sigma-1 receptors within astrocytes. A potential future experiment could entail incubating striatal slices from three different types of animals (wild-type, complete sigma-1 receptor knockout, and only expressing sigma-1 receptor in GFAP-positive astrocytes) and assessing the changes in morphology. A perhaps even simpler means of assessing the contribution of dopamine versus the sigma-1 receptor would be to conduct the present experiments in primary astrocyte culture. Since cultured astrocytes lack dopamine, it would be relatively straightforward to dissociate the effects of dopamine on astrocytic morphology and the effects of sigma-1 receptor activation on astrocytic morphology. From work in our lab, it has been observed that addition of cocaine alone to the culture medium can induce rapid stellation of astrocytes (Ortinski, unpublished observations), thus it is plausible that factors other than dopamine, particularly the sigma-1 receptor, can contribute to alterations in astrocytic morphology.

The sigma-1 receptor is a regulator of intracellular calcium dynamics (Hayashi et al., 2000; Sambo et al., 2017). Many of the initial experiments (Hayashi et al., 2000; Hayashi and Su, 2001; Hayashi and Su, 2007) exploring the molecular mechanisms of sigma-1 receptor-mediated alterations in intracellular calcium utilized the NG108 cell line, a hybrid between glioma cells (cancerous astrocytes) and neuroblastoma cells (cancerous neuronal progenitor cells), or Chinese hamster ovarian cells. While monocultures of cells are a valuable tool to study events on the molecular level, results obtained from experiments using monocultures must be considered with a grain of salt, as it is not always possible to extrapolate events that occur in culture to the situation in a living organism. For example, it is difficult to determine whether increased dopamine or sigma-1 receptor binding due to methamphetamine treatment are responsible for the alterations to astrocytic physiology. Viral transfection of astrocytes in vivo with Lck-GCaMP expressed under the GFAP promoter is a sensitive means of detecting intracellular calcium oscillations throughout the entire astrocyte (Shigetomi et al., 2013). A potential future experiment could involve incubating striatal brain slices in baths containing the treatment drugs in the present experiment and observing the effects on intracellular calcium dynamics. Addition

of selective D1 receptor antagonists to the bath could be a means of observing the contribution of signaling via the phospholipase C-stimulating D1x receptor.

BIBLIOGRAPHY

SAMHSA, (2017). Results from the 2016 National Survey on Drug Use and Health: Detailed Tables. NSDUH H-52. Rockville, MD.

Ablordeppey, S. Y., et al. (2000). "Is a nitrogen atom an important pharmacophoric element in sigma ligand binding?" Bioorganic & Medicinal Chemistry **8**(8): 2105-2111.

Aguinaga, D., et al. (2018). "Cocaine Effects on Dopaminergic Transmission Depend on a Balance between Sigma-1 and Sigma-2 Receptor Expression." Frontiers in Molecular Neuroscience **11**.

Agulhon, C., et al. (2008). "What Is the Role of Astrocyte Calcium in Neurophysiology?" Neuron **59**(6): 932-946.

Alonso, G., et al. (2000). "Immunocytochemical localization of the sigma1 receptor in the adult rat central nervous system." Neuroscience **97**(1): 155-170.

Anderson, C. M. and R. A. Swanson (2000). "Astrocyte glutamate transport: Review of properties, regulation, and physiological functions." Glia **32**(1): 1-14.

Aydar, E., et al. (2002). "The Sigma Receptor as a Ligand-Regulated Auxiliary Potassium Channel Subunit." Neuron **34**(3): 399-410.

Baker, D. A., et al. (2003). "Neuroadaptations in cystine-glutamate exchange underlie cocaine relapse." Nature Neuroscience **6**(7): 743-749.

Bergersen, L. H., et al. (2012). "Immunogold detection of L-glutamate and D-serine in small synaptic-like microvesicles in adult hippocampal astrocytes." Cerebral Cortex (New York, N.Y.: 1991) **22**(7): 1690-1697.

Besson, M. J., et al. (1969). "RELEASE OF NEWLY SYNTHESIZED DOPAMINE FROM DOPAMINE-CONTAINING TERMINALS IN THE STRIATUM OF THE RAT*." Proceedings of the National Academy of Sciences of the United States of America **62**(3): 741-748.

Beuming, T., et al. (2008). "The binding sites for cocaine and dopamine in the dopamine transporter overlap." Nature neuroscience **11**(7): 780-789.

Bezzi, P., et al. (2004). "Astrocytes contain a vesicular compartment that is competent for regulated exocytosis of glutamate." Nature Neuroscience **7**(6): 613-620.

Bindocci, E., et al. (2017). "Three-dimensional Ca2+ imaging advances understanding of astrocyte biology." Science **356**(6339).

Bogdanski, D. F. and B. B. Brodie (1969). "The effects of inorganic ions on the storage and uptake of H3-norepinephrine by rat heart slices." <u>The Journal of Pharmacology and Experimental Therapeutics</u> **165**(2): 181-189.

Boison, D., et al. (2010). "Adenosine Signalling and Function in Glial Cells." <u>Cell death and differentiation</u> **17**(7): 1071-1082.

Boitier, E., et al. (1999). "Mitochondria exert a negative feedback on the propagation of intracellular Ca2+ waves in rat cortical astrocytes." <u>The Journal of Cell Biology</u> **145**(4): 795-808.

Bolshakova, A. V., et al. (2016). "Sigma-1 receptor as a potential pharmacological target for the treatment of neuropathology." <u>St. Petersburg Polytechnical University Journal: Physics and Mathematics</u> **2**(1): 31-40.

Bowers, M. S. and P. W. Kalivas (2003). "Forebrain astroglial plasticity is induced following withdrawal from repeated cocaine administration." <u>The European Journal of Neuroscience</u> **17**(6): 1273-1278.

Brecht, M.-L. and D. Herbeck (2014). "Time to relapse following treatment for methamphetamine use: a long-term perspective on patterns and predictors." <u>Drug and alcohol dependence</u> **139**: 18-25.

Bridges, R. J., et al. (2012). "System xc- cystine/glutamate antiporter: an update on molecular pharmacology and roles within the CNS." <u>British Journal of Pharmacology</u> **165**(1): 20-34.

Broening, H. W., et al. (1997). "Methamphetamine selectively damages dopaminergic innervation to the nucleus accumbens core while sparing the shell." <u>Synapse (New York, N.Y.)</u> **27**(2): 153-160.

Brune, S., et al. (2013). "Structure of the σ1 receptor and its ligand binding site." <u>Journal of Medicinal Chemistry</u> **56**(24): 9809-9819.

Carmignoto, G., et al. (1998). "On the Role of Voltage-Dependent Calcium Channels in Calcium Signaling of Astrocytes In Situ." <u>The Journal of Neuroscience</u> **18**(12): 4637-4645.

Chai, H., et al. (2017). "Neural circuit-specialized astrocytes: transcriptomic, proteomic, morphological and functional evidence." <u>Neuron</u> **95**(3): 531-549.e539.

Cheli, V. T., et al. (2016). "L-type voltage-operated calcium channels contribute to astrocyte activation in vitro." <u>Glia</u> **64**(8): 1396-1415.

Chu, U. B. and A. E. Ruoho (2016). "Biochemical Pharmacology of the Sigma-1 Receptor." Molecular Pharmacology **89**(1): 142-153.

Covey, D. P., et al. (2013). "Amphetamine elicits opposing actions on readily releasable and reserve pools for dopamine." PLoS ONE **8**(5): e60763.

Ding, F., et al. (2013). "α1-adrenergic receptors mediate coordinated Ca2+ signaling of cortical astrocytes in awake, behaving mice." Cell calcium **54**(6).

Duan, S., et al. (2003). "P2X7 Receptor-Mediated Release of Excitatory Amino Acids from Astrocytes." The Journal of Neuroscience **23**(4): 1320-1328.

Duchen, M. R. (2000). "Mitochondria and calcium: from cell signalling to cell death." The Journal of Physiology **529**(Pt 1): 57-68.

Dunkley, P. R., et al. (2004). "Tyrosine hydroxylase phosphorylation: regulation and consequences." Journal of Neurochemistry **91**(5): 1025-1043.

Egashira, T., et al. (1987). "Effects of d-methamphetamine on monkey brain monoamine oxidase, in vivo and in vitro." Japanese Journal of Pharmacology **45**(1): 79-88.

Entrena, J. M., et al. (2016). "Sigma-1 Receptor Agonism Promotes Mechanical Allodynia After Priming the Nociceptive System with Capsaicin." Scientific Reports **6**(1): 37835.

Fellin, T., et al. (2004). "Neuronal Synchrony Mediated by Astrocytic Glutamate through Activation of Extrasynaptic NMDA Receptors." Neuron **43**(5): 729-743.

Fiacco, T. A. and K. D. McCarthy (2018). "Multiple Lines of Evidence Indicate That Gliotransmission Does Not Occur under Physiological Conditions." Journal of Neuroscience **38**(1): 3-13.

Fischer, J. F. and A. K. Cho (1979). "Chemical release of dopamine from striatal homogenates: evidence for an exchange diffusion model." The Journal of Pharmacology and Experimental Therapeutics **208**(2): 203-209.

Fischer-Smith, K. D., et al. (2012). "Differential effects of cocaine access and withdrawal on glutamate type 1 transporter expression in rat nucleus accumbens core and shell." Neuroscience **210**: 333-339.

Floor, E. and L. Meng (1996). "Amphetamine releases dopamine from synaptic vesicles by dual mechanisms." Neuroscience Letters **215**(1): 53-56.

Fontanilla, D., et al. (2009). "The Hallucinogen N,N-Dimethyltryptamine (DMT) Is an Endogenous Sigma-1 Receptor Regulator." Science (New York, N.Y.) **323**(5916): 934-937.

Francardo, V., et al. (2014). "Pharmacological stimulation of sigma-1 receptors has neurorestorative effects in experimental parkinsonism." Brain: A Journal of Neurology **137**(Pt 7): 1998-2014.

Fraser, R., et al. (2014). "An N-Terminal Threonine Mutation Produces an Efflux-Favorable, Sodium-Primed Conformation of the Human Dopamine Transporter." Molecular Pharmacology **86**(1): 76-85.

Freyberg, Z., et al. (2016). "Mechanisms of amphetamine action illuminated through optical monitoring of dopamine synaptic vesicles in Drosophila brain." Nature Communications **7**.

Fu, Y., et al. (2010). "Sigma-1 receptors amplify dopamine D1 receptor signaling at presynaptic sites in the prelimbic cortex." Biochimica Et Biophysica Acta **1803**(12): 1396-1408.

Fujita, T., et al. (2014). "Neuronal Transgene Expression in Dominant-Negative SNARE Mice." The Journal of Neuroscience **34**(50): 16594-16604.

Fung, Y. K. and N. J. Uretsky (1982). "The importance of calcium in the amphetamine-induced stimulation of dopamine synthesis in mouse striata in vivo." Journal of Pharmacology and Experimental Therapeutics **223**(2): 477-482.

Gallagher, C. J. and M. W. Salter (2003). "Differential Properties of Astrocyte Calcium Waves Mediated by P2Y1 and P2Y2 Receptors." Journal of Neuroscience **23**(17): 6728-6739.

Galloway, A., et al. (2018). "Dopamine Triggers CTCF-Dependent Morphological and Genomic Remodeling of Astrocytes." The Journal of Neuroscience: The Official Journal of the Society for Neuroscience **38**(21): 4846-4858.

Gnegy, M. E., et al. (2004). "Intracellular Ca2+ regulates amphetamine-induced dopamine efflux and currents mediated by the human dopamine transporter." Molecular Pharmacology **66**(1): 137-143.

Gromek, K. A., et al. (2014). "The Oligomeric States of the Purified Sigma-1 Receptor Are Stabilized by Ligands." The Journal of Biological Chemistry **289**(29): 20333-20344.

Hanner, M., et al. (1996). "Purification, molecular cloning, and expression of the mammalian sigma1-binding site." Proceedings of the National Academy of Sciences of the United States of America **93**(15): 8072-8077.

Hardingham, G. E. and H. Bading (2010). "Synaptic versus extrasynaptic NMDA receptor signalling: implications for neurodegenerative disorders." Nature reviews. Neuroscience **11**(10): 682-696.

Hasbi, A., et al. (2010). "Heteromerization of dopamine D2 receptors with dopamine D1 or D5 receptors generates intracellular calcium signaling by different mechanisms." Current opinion in pharmacology **10**(1): 93.

Hayashi, T. (2019). "The Sigma-1 Receptor in Cellular Stress Signaling." Frontiers in Neuroscience **13**.

Hayashi, T., et al. (2000). "Ca(2+) signaling via sigma(1)-receptors: novel regulatory mechanism affecting intracellular Ca(2+) concentration." The Journal of Pharmacology and Experimental Therapeutics **293**(3): 788-798.

Hayashi, T. and T.-P. Su (2001). "Regulating ankyrin dynamics: Roles of sigma-1 receptors." Proceedings of the National Academy of Sciences **98**(2): 491-496.

Hayashi, T. and T.-P. Su (2003). "σ-1 Receptors (σ1 Binding Sites) Form Raft-Like Microdomains and Target Lipid Droplets on the Endoplasmic Reticulum: Roles in Endoplasmic Reticulum Lipid Compartmentalization and Export." Journal of Pharmacology and Experimental Therapeutics **306**(2): 718-725.

Hayashi, T. and T.-P. Su (2007). "Sigma-1 receptor chaperones at the ER-mitochondrion interface regulate Ca(2+) signaling and cell survival." Cell **131**(3): 596-610.

Hedges, D. M., et al. (2018). "Methamphetamine Induces Dopamine Release in the Nucleus Accumbens Through a Sigma Receptor-Mediated Pathway." Neuropsychopharmacology: Official Publication of the American College of Neuropsychopharmacology **43**(6): 1405-1414.

Hellewell, S. B. and W. D. Bowen (1990). "A sigma-like binding site in rat pheochromocytoma (PC12) cells: decreased affinity for (+)-benzomorphans and lower molecular weight suggest a different sigma receptor form from that of guinea pig brain." Brain Research **527**(2): 244-253.

Hertz, L., et al. (1999). "Astrocytes: Glutamate producers for neurons." Journal of Neuroscience Research **57**(4): 417-428.

Hiranita, T. and Z. Freyberg (2016). "Importance of Substrate-Coupled Proton Antiport by the Vesicular Monoamine Transporter in the Actions of Amphetamines in Drosophila Brain." Journal of alcoholism and drug dependence **4**(6).

Hol, E. M., et al. (2003). "Neuronal expression of GFAP in patients with Alzheimer pathology and identification of novel GFAP splice forms." Molecular Psychiatry **8**(9): 786-796.

Hong, W. C., et al. (2017). "The sigma-1 receptor modulates dopamine transporter conformation and cocaine binding and may thereby potentiate cocaine self-administration in rats." The Journal of Biological Chemistry **292**(27): 11250-11261.

Hu, G., et al. (2013). "New Fluorescent Substrate Enables Quantitative and High-Throughput Examination of Vesicular Monoamine Transporter 2 (VMAT2)." ACS Chemical Biology **8**(9): 1947-1954.

Johnson, L. A. A., et al. (2005). "Regulation of Amphetamine-stimulated Dopamine Efflux by Protein Kinase C β." Journal of Biological Chemistry **280**(12): 10914-10919.

Jones, C. M., et al. (2020). "Resurgent Methamphetamine Use at Treatment Admission in the United States, 2008–2017." American Journal of Public Health **110**(4): 509-516.

Kahlig, K. M., et al. (2005). "Amphetamine induces dopamine efflux through a dopamine transporter channel." Proceedings of the National Academy of Sciences of the United States of America **102**(9): 3495-3500.

Khan, M. T., et al. (2019). "Astrocytic rather than neuronal P2X7 receptors modulate the function of the tri-synaptic network in the rodent hippocampus." Brain Research Bulletin **151**: 164-173.

Khoshbouei, H., et al. (2003). "Amphetamine-induced dopamine efflux. A voltage-sensitive and intracellular Na+-dependent mechanism." The Journal of Biological Chemistry **278**(14): 12070-12077.

Kim, F. J., et al. (2010). "Sigma 1 receptor modulation of G-protein-coupled receptor signaling: potentiation of opioid transduction independent from receptor binding." Molecular Pharmacology **77**(4): 695-703.

Kofuji, P. and E. A. Newman (2004). "POTASSIUM BUFFERING IN THE CENTRAL NERVOUS SYSTEM." Neuroscience **129**(4): 1045-1056.

Kovács, A. and B. Pál (2017). "Astrocyte-Dependent Slow Inward Currents (SICs) Participate in Neuromodulatory Mechanisms in the Pedunculopontine Nucleus (PPN)." Frontiers in Cellular Neuroscience **11**.

Kuczenski, R. (1975). "Effects of catecholamine releasing agents on synaptosomal dopamine biosynthesis: Multiple pools of dopamine or multiple forms of tyrosine hydroxylase?" Neuropharmacology **14**(1): 1-10.

Lee, M., et al. (2010). "Development of pH Responsive Fluorescent False Neurotransmitters." Journal of the American Chemical Society **132**(26): 8828-8830.

Liang, N. Y. and C. O. Rutledge (1982). "Comparison of the release of [3H]dopamine from isolated corpus striatum by amphetamine, fenfluramine and unlabelled dopamine." Biochemical Pharmacology **31**(6): 983-992.

Liddelow, S. A. and B. A. Barres (2017). "Reactive Astrocytes: Production, Function, and Therapeutic Potential." Immunity **46**(6): 957-967.

Liu, J., et al. (2009). "Activation of phosphatidylinositol-linked novel D1 dopamine receptor contributes to the calcium mobilization in cultured rat prefrontal cortical astrocytes." Cellular and Molecular Neurobiology **29**(3): 317-328.

Liu, J.-F. and J.-X. Li (2018). "TAAR1 in Addiction: Looking Beyond the Tip of the Iceberg." Frontiers in Pharmacology **9**.

Loland, C. J., et al. (2008). "Relationship between Conformational Changes in the Dopamine Transporter and Cocaine-Like Subjective Effects of Uptake Inhibitors." Molecular Pharmacology **73**(3): 813-823.

Mack, F. and H. Bönisch (1979). "Dissociation constants and lipophilicity of catecholamines and related compounds." Naunyn-Schmiedeberg's Archives of Pharmacology **310**(1): 1-9.

Mager, S., et al. (1994). "Conducting states of a mammalian serotonin transporter." Neuron **12**(4): 845-859.

Mantle, T. J., et al. (1976). "Inhibition of monoamine oxidase by amphetamine and related compounds." Biochemical Pharmacology **25**(18): 2073-2077.

Mariotti, L., et al. (2016). "The inhibitory neurotransmitter GABA evokes long-lasting Ca(2+) oscillations in cortical astrocytes." Glia **64**(3): 363-373.

Martin, W. R., et al. (1976). "The effects of morphine- and nalorphine- like drugs in the nondependent and morphine-dependent chronic spinal dog." The Journal of Pharmacology and Experimental Therapeutics **197**(3): 517-532.

Matsumoto, R. R., et al. (2002). "Involvement of sigma receptors in the behavioral effects of cocaine: evidence from novel ligands and antisense oligodeoxynucleotides." Neuropharmacology **42**(8): 1043-1055.

Matsumoto, R. R. and B. Pouw (2000). "Correlation between neuroleptic binding to σ1 and σ2 receptors and acute dystonic reactions." European Journal of Pharmacology **401**(2): 155-160.

Mavlyutov, T. A. and A. E. Ruoho (2007). "Ligand-dependent localization and intracellular stability of sigma-1 receptors in CHO-K1 cells." Journal of Molecular Signaling **2**: 8.

Melikian, H. E. and K. M. Buckley (1999). "Membrane trafficking regulates the activity of the human dopamine transporter." The Journal of Neuroscience: The Official Journal of the Society for Neuroscience **19**(18): 7699-7710.

Mittelsteadt, T., et al. (2009). "Differential mRNA expression patterns of the synaptotagmin gene family in the rodent brain." The Journal of Comparative Neurology **512**(4): 514-528.

Moebius, F. F., et al. (1997). "High affinity of sigma 1-binding sites for sterol isomerization inhibitors: evidence for a pharmacological relationship with the yeast sterol C8-C7 isomerase." British Journal of Pharmacology **121**(1): 1-6.

Mori, T., et al. (2013). "Sigma-1 Receptor Chaperone at the ER-Mitochondrion Interface Mediates the Mitochondrion-ER-Nucleus Signaling for Cellular Survival." PLoS ONE **8**(10).

Moye, S. L., et al. (2019). "Visualizing Astrocyte Morphology Using Lucifer Yellow Iontophoresis." JoVE (Journal of Visualized Experiments)(151): e60225.

Mundorf, M. L., et al. (1999). "Amine weak bases disrupt vesicular storage and promote exocytosis in chromaffin cells." Journal of Neurochemistry **73**(6): 2397-2405.

Nakagawa, T., et al. (2011). "Repeated Exposure to Methamphetamine, Cocaine or Morphine Induces Augmentation of Dopamine Release in Rat Mesocorticolimbic Slice Co-Cultures." PLoS ONE **6**(9).

Narita, M., et al. (2005). "Long-lasting change in brain dynamics induced by methamphetamine: enhancement of protein kinase C-dependent astrocytic response and behavioral sensitization." Journal of Neurochemistry **93**(6): 1383-1392.

Navarrete, M. and A. Araque (2008). "Endocannabinoids mediate neuron-astrocyte communication." Neuron **57**(6): 883-893.

Navarro, G., et al. (2010). "Direct involvement of sigma-1 receptors in the dopamine D1 receptor-mediated effects of cocaine." Proceedings of the National Academy of Sciences of the United States of America **107**(43): 18676-18681.

Navarro, G., et al. (2013). "Cocaine Inhibits Dopamine D2 Receptor Signaling via Sigma-1-D2 Receptor Heteromers." PLoS ONE **8**(4): e61245.

Nguyen, E. C., et al. (2005). "Involvement of sigma (sigma) receptors in the acute actions of methamphetamine: receptor binding and behavioral studies." Neuropharmacology **49**(5): 638-645.

Nguyen, L., et al. (2014). "Involvement of sigma-1 receptors in the antidepressant-like effects of dextromethorphan." PLoS ONE **9**(2): e89985.

Nicosia, N., et al. (2009). The Costs of Methamphetamine Use: A National Estimate. Santa Monica, CA, RAND Corporation.

Nielsen, A. K., et al. (2019). "Substrate-induced conformational dynamics of the dopamine transporter." Nature Communications **10**.

Nizar, K., et al. (2013). "In vivo stimulus-induced vasodilation occurs without IP3 receptor activation and may precede astrocytic calcium increase." The Journal of Neuroscience: The Official Journal of the Society for Neuroscience **33**(19): 8411-8422.

Novakova, M., et al. (1998). "Highly selective σ receptor ligands elevate inositol 1,4,5-trisphosphate production in rat cardiac myocytes." European Journal of Pharmacology **353**(2): 315-327.

Ortinski, P. I., et al. (2013). "Extrasynaptic Targeting of NMDA Receptors Following D1 Dopamine Receptor Activation and Cocaine Self-Administration." The Journal of Neuroscience **33**(22): 9451-9461.

Pal, A., et al. (2008). "Juxtaposition of the Steroid Binding Domain-like I and II Regions Constitutes a Ligand Binding Site in the σ-1 Receptor." Journal of Biological Chemistry **283**(28): 19646-19656.

Pál, B. (2015). "Astrocytic Actions on Extrasynaptic Neuronal Currents." Frontiers in Cellular Neuroscience **9**.

Panenka, W., et al. (2001). "P2X7-Like Receptor Activation in Astrocytes Increases Chemokine Monocyte Chemoattractant Protein-1 Expression via Mitogen-Activated Protein Kinase." Journal of Neuroscience **21**(18): 7135-7142.

Parnis, J., et al. (2013). "Mitochondrial Exchanger NCLX Plays a Major Role in the Intracellular Ca2+ Signaling, Gliotransmission, and Proliferation of Astrocytes." The Journal of Neuroscience **33**(17): 7206-7219.

Parpura, V. and P. G. Haydon (2000). "Physiological astrocytic calcium levels stimulate glutamate release to modulate adjacent neurons." Proceedings of the National Academy of Sciences of the United States of America **97**(15): 8629-8634.

Parri, H. R. and V. Crunelli (2003). "The role of Ca2+ in the generation of spontaneous astrocytic Ca2+ oscillations." Neuroscience **120**(4): 979-992.

Parsegian, A. and R. E. See (2014). "Dysregulation of Dopamine and Glutamate Release in the Prefrontal Cortex and Nucleus Accumbens Following Methamphetamine Self-

Administration and During Reinstatement in Rats." <u>Neuropsychopharmacology</u> **39**(4): 811-822.

Peter, D., et al. (1994). "The chromaffin granule and synaptic vesicle amine transporters differ in substrate recognition and sensitivity to inhibitors." <u>The Journal of Biological Chemistry</u> **269**(10): 7231-7237.

Peter, D., et al. (1995). "Differential expression of two vesicular monoamine transporters." <u>The Journal of Neuroscience: The Official Journal of the Society for Neuroscience</u> **15**(9): 6179-6188.

Petravicz, J., et al. (2014). "Astrocyte IP3R2-dependent Ca(2+) signaling is not a major modulator of neuronal pathways governing behavior." <u>Frontiers in Behavioral Neuroscience</u> **8**: 384.

Petrelli, F., et al. (2020). "Dysfunction of homeostatic control of dopamine by astrocytes in the developing prefrontal cortex leads to cognitive impairments." <u>Molecular Psychiatry</u> **25**(4): 732-749.

Pifl, C., et al. (1995). "Mechanism of the dopamine-releasing actions of amphetamine and cocaine: plasmalemmal dopamine transporter versus vesicular monoamine transporter." <u>Molecular Pharmacology</u> **47**(2): 368-373.

Pinton, P., et al. (2008). "Calcium and apoptosis: ER-mitochondria Ca2+ transfer in the control of apoptosis." <u>Oncogene</u> **27**(50): 6407-6418.

Pothos, E. N., et al. (2002). "Stimulation-dependent regulation of the pH, volume and quantal size of bovine and rodent secretory vesicles." <u>The Journal of Physiology</u> **542**(Pt 2): 453-476.

Ransohoff, R. M. (2016). "A polarizing question: do M1 and M2 microglia exist?" <u>Nature Neuroscience</u> **19**(8): 987-991.

Reichenbach, A., et al. (2010). "Morphology and dynamics of perisynaptic glia." <u>Brain Research Reviews</u> **63**(1-2): 11-25.

Ritz, M. C., et al. (1987). "Cocaine receptors on dopamine transporters are related to self-administration of cocaine." <u>Science (New York, N.Y.)</u> **237**(4819): 1219-1223.

Rivière, G. J., et al. (2000). "Disposition of Methamphetamine and Its Metabolite Amphetamine in Brain and Other Tissues in Rats after Intravenous Administration." <u>Journal of Pharmacology and Experimental Therapeutics</u> **292**(3): 1042-1047.

Robinson, J. B. (1985). "Stereoselectivity and isoenzyme selectivity of monoamine oxidase inhibitors. Enantiomers of amphetamine, N-methylamphetamine and deprenyl." <u>Biochemical Pharmacology</u> **34**(23): 4105-4108.

Rodvelt, K. R., et al. (2011). "The sigma receptor agonist SA4503 both attenuates and enhances the effects of methamphetamine." <u>Drug and alcohol dependence</u> **116**(1-3): 203-210.

Romero, L., et al. (2012). "Pharmacological properties of S1RA, a new sigma-1 receptor antagonist that inhibits neuropathic pain and activity-induced spinal sensitization." <u>British Journal of Pharmacology</u> **166**(8): 2289-2306.

Romieu, P., et al. (2002). "Involvement of the Sigma 1 Receptor in Cocaine-induced Conditioned Place Preference: Possible Dependence on Dopamine Uptake Blockade." <u>Neuropsychopharmacology</u> **26**(4): 444-455.

Rose, C. R., et al. (2018). "Astroglial Glutamate Signaling and Uptake in the Hippocampus." <u>Frontiers in Molecular Neuroscience</u> **10**.

Sambo, D. O., et al. (2017). "The sigma-1 receptor modulates methamphetamine dysregulation of dopamine neurotransmission." <u>Nature Communications</u> **8**(1): 2228.

Savtchouk, I. and A. Volterra (2018). "Gliotransmission: Beyond Black-and-White." <u>Journal of Neuroscience</u> **38**(1): 14-25.

Schiweck, J., et al. (2018). "Important Shapeshifter: Mechanisms Allowing Astrocytes to Respond to the Changing Nervous System During Development, Injury and Disease." <u>Frontiers in Cellular Neuroscience</u> **12**.

Schmidt, H. R., et al. (2018). "Structural basis for σ 1 receptor ligand recognition." <u>Nature Structural & Molecular Biology</u> **25**(10): 981-987.

Schmidt, H. R., et al. (2016). "Crystal structure of the human σ1 receptor." <u>Nature</u> **532**(7600): 527-530.

Schousboe, A. (2003). "Role of Astrocytes in the Maintenance and Modulation of Glutamatergic and GABAergic Neurotransmission." <u>Neurochemical Research</u> **28**(2): 347-352.

Schuldiner, S., et al. (1995). "Vesicular neurotransmitter transporters: from bacteria to humans." <u>Physiological Reviews</u> **75**(2): 369-392.

Scobie, K. N., et al. (2014). "Essential role of poly(ADP-ribosyl)ation in cocaine action." <u>Proceedings of the National Academy of Sciences</u> **111**(5): 2005-2010.

Scofield, M. D., et al. (2016). "Cocaine self-administration and extinction leads to reduced GFAP expression and morphometric features of astrocytes in the nucleus accumbens core." <u>Biological psychiatry</u> **80**(3): 207-215.

Scofield Michael, D., et al. (2015). "Gq-DREADD Selectively Initiates Glial Glutamate Release and Inhibits Cue-induced Cocaine Seeking." Biological psychiatry **78**(7): 441-451.

Seth, P., et al. (2001). "Expression pattern of the type 1 sigma receptor in the brain and identity of critical anionic amino acid residues in the ligand-binding domain of the receptor." Biochimica Et Biophysica Acta **1540**(1): 59-67.

Sherwood, M. W., et al. (2017). "Astrocytic IP3 Rs: Contribution to Ca2+ signalling and hippocampal LTP." Glia **65**(3): 502-513.

Shigetomi, E., et al. (2013). "Imaging calcium microdomains within entire astrocyte territories and endfeet with GCaMPs expressed using adeno-associated viruses." The Journal of General Physiology **141**(5): 633-647.

Shigetomi, E., et al. (2011). "TRPA1 channels regulate astrocyte resting calcium and inhibitory synapse efficacy through GAT-3." Nature Neuroscience **15**(1): 70-80.

Sidiropoulou, K., et al. (2001). "Amphetamine administration does not alter protein levels of the GLT-1 and EAAC1 glutamate transporter subtypes in rat midbrain, nucleus accumbens, striatum, or prefrontal cortex." Brain Research. Molecular Brain Research **90**(2): 187-192.

Siemsen, B. M., et al. (2019). "Effects of Methamphetamine Self-Administration and Extinction on Astrocyte Structure and Function in the Nucleus Accumbens Core." Neuroscience **406**: 528-541.

Simmler, L. D., et al. (2013). "Bupropion, methylphenidate, and 3,4-methylenedioxypyrovalerone antagonize methamphetamine-induced efflux of dopamine according to their potencies as dopamine uptake inhibitors: implications for the treatment of methamphetamine dependence." BMC Research Notes **6**: 220.

Sonders, M. S., et al. (1997). "Multiple ionic conductances of the human dopamine transporter: the actions of dopamine and psychostimulants." The Journal of Neuroscience: The Official Journal of the Society for Neuroscience **17**(3): 960-974.

Srinivasan, R., et al. (2015). "Ca(2+) signaling in astrocytes from Ip3r2(-/-) mice in brain slices and during startle responses in vivo." Nature Neuroscience **18**(5): 708-717.

Srivats, S., et al. (2016). "Sigma1 receptors inhibit store-operated Ca2+ entry by attenuating coupling of STIM1 to Orai1." The Journal of Cell Biology **213**(1): 65-79.

Stein, W. H. (1967). The Movement of Molecules Across Cell Membranes, Elsevier.

Su, T. P. (1982). "Evidence for sigma opioid receptor: binding of [3H]SKF-10047 to etorphine-inaccessible sites in guinea-pig brain." Journal of Pharmacology and Experimental Therapeutics **223**(2): 284-290.

Su, T. P. and T. Hayashi (2001). "Cocaine affects the dynamics of cytoskeletal proteins via sigma(1) receptors." Trends in Pharmacological Sciences **22**(9): 456-458.

Su, T. P., et al. (1988). "Steroid binding at sigma receptors suggests a link between endocrine, nervous, and immune systems." Science (New York, N.Y.) **240**(4849): 219-221.

Suadicani, S. O., et al. (2006). "P2X7 Receptors Mediate ATP Release and Amplification of Astrocytic Intercellular Ca2+ Signaling." The Journal of Neuroscience **26**(5): 1378-1385.

Sulzer, D. (2011). "How Addictive Drugs Disrupt Presynaptic Dopamine Neurotransmission." Neuron **69**(4): 628-649.

Sulzer, D., et al. (1995). "Amphetamine redistributes dopamine from synaptic vesicles to the cytosol and promotes reverse transport." The Journal of Neuroscience: The Official Journal of the Society for Neuroscience **15**(5 Pt 2): 4102-4108.

Sun, W., et al. (2013). "Glutamate-Dependent Neuroglial Calcium Signaling Differs Between Young and Adult Brain." Science (New York, N.Y.) **339**(6116): 197-200.

Suzuki, O., et al. (1980). "Inhibition of monoamine oxidase by d-methamphetamine." Biochemical Pharmacology **29**(14): 2071-2073.

Szumlinski, K. K., et al. (2017). "Methamphetamine Addiction Vulnerability: The Glutamate, the Bad, and the Ugly." Biological Psychiatry **81**(11): 959-970.

Tainter, M. L. and D. K. Chang (1927). "The Antagonism of the Pressor Action of Tyramine by Cocaine." Journal of Pharmacology and Experimental Therapeutics **30**(3): 193-207.

Takahashi, S., et al. (2000). "Involvement of sigma 1 receptors in methamphetamine-induced behavioral sensitization in rats." Neuroscience Letters **289**(1): 21-24.

Takeuchi, A., et al. (2015). "The destiny of Ca2+ released by mitochondria." The Journal of Physiological Sciences **65**: 11-24.

Tanaka, T., et al. (1991). "Ca2(+)-dependent regulation of the spectrin/actin interaction by calmodulin and protein 4.1." The Journal of Biological Chemistry **266**(2): 1134-1140.

Testen, A., et al. (2020). "High-Resolution Three-Dimensional Imaging of Individual Astrocytes Using Confocal Microscopy." Current Protocols in Neuroscience **91**(1): e92.

Testen, A., et al. (2018). "Region-Specific Reductions in Morphometric Properties and Synaptic Colocalization of Astrocytes Following Cocaine Self-Administration and Extinction." <u>Frontiers in Cellular Neuroscience</u> **12**.

Tong, X., et al. (2012). "Genetically Encoded Calcium Indicators and Astrocyte Calcium Microdomains." <u>The Neuroscientist</u>.

Tsai, S.-Y., et al. (2009). "Sigma-1 receptors regulate hippocampal dendritic spine formation via a free radical-sensitive mechanism involving Rac1xGTP pathway." <u>Proceedings of the National Academy of Sciences of the United States of America</u> **106**(52): 22468-22473.

Underhill, S. M., et al. (2019). "Amphetamines signal through intracellular TAAR1 receptors coupled to Gα 13 and Gα S in discrete subcellular domains." <u>Molecular Psychiatry</u>: 1-16.

Verkhratsky, A. and C. Steinhäuser (2000). "Ion channels in glial cells." <u>Brain Research Reviews</u> **32**(2): 380-412.
Verkhratsky, A. and M. Nedergaard (2018). "Physiology of Astroglia." <u>Physiological Reviews</u> **98**(1): 239-389.

Wang, H. Y., et al. (1995). "Evidence for the coupling of Gq protein to D1-like dopamine sites in rat striatum: possible role in dopamine-mediated inositol phosphate formation." <u>Molecular Pharmacology</u> **48**(6): 988-994.

Wang, K. H., et al. (2015). "Neurotransmitter and psychostimulant recognition by the dopamine transporter." <u>Nature</u> **521**(7552): 322-327.

Wolfes, A. C., et al. (2017). "A novel method for culturing stellate astrocytes reveals spatially distinct Ca2+ signaling and vesicle recycling in astrocytic processes." <u>The Journal of General Physiology</u> **149**(1): 149-170.

Xie, Z. and G. M. Miller (2007). "Trace amine-associated receptor 1 is a modulator of the dopamine transporter." <u>The Journal of Pharmacology and Experimental Therapeutics</u> **321**(1): 128-136.

Xie, Z. and G. M. Miller (2009). "A Receptor Mechanism for Methamphetamine Action in Dopamine Transporter Regulation in Brain." <u>The Journal of Pharmacology and Experimental Therapeutics</u> **330**(1): 316-325.

Yamamoto, H., et al. (1999). "Amino acid residues in the transmembrane domain of the type 1 sigma receptor critical for ligand binding." <u>FEBS letters</u> **445**(1): 19-22.

Yasui, Y. and T.-P. Su (2016). "Potential Molecular Mechanisms on the Role of the Sigma-1 Receptor in the Action of Cocaine and Methamphetamine." Journal of drug and alcohol research **5**.

Zaczek, R., et al. (1991). "Interactions of [3H]amphetamine with rat brain synaptosomes. II. Active transport." The Journal of Pharmacology and Experimental Therapeutics **257**(2): 830-835.

Zhang, K., et al. (2017). "Sigma-1 Receptor Plays a Negative Modulation on N-type Calcium Channel." Frontiers in Pharmacology **8**.

Zhang, X., et al. (2018). "Striatal Tyrosine Hydroxylase Is Stimulated via TAAR1 by 3-Iodothyronamine, But Not by Tyramine or β-Phenylethylamine." Frontiers in Pharmacology **9**.

Zhang, Y., et al. (2001). "Comparison of cocaine- and methamphetamine-evoked dopamine and glutamate overflow in somatodendritic and terminal field regions of the rat brain during acute, chronic, and early withdrawal conditions." Annals of the New York Academy of Sciences **937**: 93-120.

Zhang, Y., et al. (2015). "Involvement of sigma-1 receptor in astrocyte activation induced by methamphetamine via up-regulation of its own expression." Journal of Neuroinflammation **12**: 29.

Zonta, M., et al. (2003). "Neuron-to-astrocyte signaling is central to the dynamic control of brain microcirculation." Nature Neuroscience **6**(1): 43-50.

VITA

RICHIK NEOGI

EDUCATION

Bachelor of Science in Neuroscience from Washington State University Vancouver

ACADEMIC EMPLOYMENT

Research Assistant to Dr. Summer Gibbs, Department of Biomedical Engineering, Oregon Health Sciences University. Summer 2013-Summer 2014

Research Assistant to Dr. Michael Morgan, Department of Neuroscience, Washington State University Vancouver, Winter 2018-Summer 2018

PRESENTATIONS AT PROFESSIONAL MEETINGS

Neogi, R and Morgan, M.M., "Microglial P2X4 Receptors Contribute to Morphine Tolerance Mediated by the Periaqueductal Gray" at the International Narcotics Research Conference, July 2019, New York, NY

ACADEMIC AWARDS

Recipient of funding from WSU Alcohol and Drug Research Program